© 2019. Published by The Company of Biologists Ltd | Development (2019) 146, dev175919. doi:10.1242/dev.175919

RESEARCH ARTICLE

Root gravity response module guides differential growth determining both root bending and apical hook formation in *Arabidopsis*

Qiang Zhu[1,2,*], Marçal Gallemí[2,*], Jiří Pospíšil[3], Petra Žádníková[4], Miroslav Strnad[3] and Eva Benková[2,‡]

ABSTRACT

The apical hook is a transiently formed structure that plays a protective role when the germinating seedling penetrates through the soil towards the surface. Crucial for proper bending is the local auxin maxima, which defines the concave (inner) side of the hook curvature. As no sign of asymmetric auxin distribution has been reported in embryonic hypocotyls prior to hook formation, the question of how auxin asymmetry is established in the early phases of seedling germination remains largely unanswered. Here, we analyzed the auxin distribution and expression of PIN auxin efflux carriers from early phases of germination, and show that bending of the root in response to gravity is the crucial initial cue that governs the hypocotyl bending required for apical hook formation. Importantly, polar auxin transport machinery is established gradually after germination starts as a result of tight root-hypocotyl interaction and a proper balance between abscisic acid and gibberellins.

This article has an associated 'The people behind the papers' interview.

KEY WORDS: Apical hook, Formation stage, Auxin maxima, Root gravitropism, *Arabidopsis*, Green embryos

INTRODUCTION

Multicellular organisms have evolved mechanisms for the protection of cells that are essential for their survival. In dicot plants, the apical hook, which results from differential cell growth on two sides of the hypocotyl, has evolved to protect the delicate shoot meristem as the seedling approaches the soil surface (Darwin and Darwin, 1881; Raz and Ecker, 1999). By gradual bending of the apical part of the hypocotyl, the hook is formed soon after germination; it is maintained in a closed state while the hypocotyl continues to penetrate through the soil, and rapidly opens when exposed to the light in proximity of the soil surface (Vandenbussche et al., 2010; Žádníková et al., 2010).

Plant hormones, including auxin, play an important role in the regulation of apical hook development (Stepanova et al., 2008; Vandenbussche et al., 2010; Žádníková et al., 2010; Mazzella et al., 2014). Defects in auxin metabolism, transport and signaling dramatically affect all phases of apical hook growth (Gallego-Bartolomé et al., 2011; Abbas et al., 2013). In particular, asymmetric auxin distribution is linked with differential cell growth and proper apical hook development (Kuhn and Galston, 1992; Vandenbussche et al., 2010; Žádníková et al., 2010, 2016). Local auxin accumulation is indispensable for hook bending, and chemical or genetic inhibition of polar auxin transport severely interferes with apical hook development (Friml et al., 2002; Forner and Binder, 2007). Dynamic auxin distribution is tightly controlled by polar auxin transport, involving mainly AUXIN/AUXIN-LIKE (AUX/LAX) influx proteins and PIN-FORMED (PIN) efflux carriers (Petrasek and Friml, 2009; Vandenbussche et al., 2010; Žádníková et al., 2010; Cho and Cho, 2012; Swarup and Péret, 2012). Analysis of expression and membrane localization of auxin carriers suggests that auxin from the central cylinder is redirected through the endodermis towards the cortex and epidermis in the upper part of the hypocotyl, and afterwards, in the epidermis layer, redistributed to the inner side of the hook. Several PIN proteins, including PIN3, PIN4 and PIN7, are involved in this process. Mutations in these PIN genes led to specific defects in apical hook development. It has been proposed that the higher abundance of PIN3 and PIN4 at the cell membrane on the convex (outer) side compared with the concave (inner) side of the apical hook might enhance the draining of auxin from the outer cortex and epidermal layers and the formation of an auxin maximum at the concave side (Fig. S1A; Žádníková et al., 2010). Indeed, mathematical modeling of auxin transport dynamics, based on the observed PIN expression pattern, supports this model (Žádníková et al., 2016).

Although much progress has been made in apical hook development research, several key questions, such as what is the mechanism that determines the apical hook formation, remain unanswered. As no sign of asymmetric auxin distribution was reported prior to hook bending, the question arises of how asymmetry of auxin distribution is established in the early phases of seedling growth. Here, we show that bending of the root in response to gravity, which is driven by auxin accumulating at the gravi-stimulated side, is the initial cue coordinating formation of the apical hook. Interference with the gravity response of the root, either by genetic or mechanical means, affects hook formation. Accordingly, after germination is initiated, the polar auxin transport machinery that mediates the root gravity response is gradually established to align root growth with the gravi-stimulus. Importantly, during these early phases of germination, expression of the auxin efflux carrier *PIN2* extends beyond the root border and, thus, at the gravi-stimulated side, the auxin maximum extends into hypocotyl. Such an enlarged auxin maximum might promote

[1]Basic Forestry & Proteomics Center (BFPC), College of Forestry, Fujian Agriculture and Forestry University, 350002 Fuzhou, China. [2]Institute of Science and Technology Austria, Klosterneuburg, 3400, Austria. [3]Laboratory of Growth Regulators, Institute of Experimental Botany ASCR & Palacký University Olomouc, CZ-771 47, Czech Republic. [4]Department of Plant Systems Biology, VIB, 9052 Gent, Belgium.
*These authors contributed equally to this work

‡Author for correspondence (eva.benkova@ist.ac.at)

M.G., 0000-0003-4675-6893; J.P., 0000-0002-0198-8116; E.B., 0000-0002-8510-9739

Received 16 January 2019; Accepted 23 July 2019

Development (2019) 146, dev175919. doi:10.1242/dev.175919

differential growth of both root and hypocotyl cells and trigger initial bending of the hypocotyl. We propose that this primary differential cell growth at the base of the hypocotyl might contribute to the establishment of a regulatory feedback loop that reinforces an axial asymmetry of polar auxin transport that governs hypocotyl bending and formation of the hook. Our study demonstrates that apical hook formation is the result of tight root-hypocotyl communication when the initial stimulus originating from root bending is transmitted and perceived by the hypocotyl. We show that a tight balance between abscisic acid (ABA) and gibberellins (GA), two principal hormonal regulators of seed maturation and germination (Nambara et al., 1995; Delmas et al., 2013; Liu and Hou, 2018), is crucial to preset hypocotyls for proper root-hypocotyl communication, which is required for apical hook formation.

RESULTS

Bending of the mature embryo in the seed coat does not pre-determine apical hook formation

The origin of the hypocotyl asymmetry that leads to apical hook formation is still unknown. Prior to germination, the *Arabidopsis* mature embryo is curled up in typical 'U' shape with the two cotyledons bent over as a result of seed coat mechanical constraints (Fig. S1B). We questioned whether this asymmetry is transmitted to apical hook formation in course of seedling germination. To explore whether embryonic shape acts as a regulatory cue for apical hook formation, mature embryos were excised from their seed coats and positioned on media in an orientated manner either root-downwards (embryo in a 'Ω' shape with both root and cotyledon poles facing downwards), or root-upwards (embryo in a 'U' shape with both root and cotyledon poles facing upwards; Fig. S1B, Fig. 1A,B), and apical hook formation during germination was examined. If embryo shape is decisive for hook curvature, then hook curvature should match the original embryonic bending regardless of orientation on the medium. Monitoring apical hook formation in real time revealed that embryos in the root-downwards position formed the apical hook that followed the embryo shape (Fig. 1A, Movie 1). However, germination of seedlings in the root-upwards position led to apical hook formation opposite to the original 'U' structure of the embryo (Fig. 1B, Movie 2). This result suggests that the shape of the mature embryo is not decisive for apical hook bending. However, observation of seedlings germinating from embryos in the root-upwards position indicated that growth and bending of the root in response to gravity might coordinate formation of the apical hook.

Gravity-driven bending of the embryonic root coordinates apical hook formation

Germination of seedlings starts by outgrowth of the embryonic root and its proper alignment with the gravity vector. To explore the role of the embryonic root in apical hook development, we tracked hook curvature formation during seedling germination after dissection of the embryonic root. Monitoring of root-less seedling development in real time revealed severe defects in the formation of the apical hook. Frequently, these seedlings were either unable to form fully closed apical hooks, or apical hooks were formed with significant delays and were maintained for a shorter time compared with control seedlings with intact roots (Fig. S1C,D). To corroborate the role of root gravitropism in the coordination of apical hook formation, we searched for molecular factors that specifically control the root gravity response but are not otherwise involved in growth and developmental processes in etiolated seedlings. The *PIN2* auxin efflux carrier, a key component of the root gravitropic response expression of which is restricted to the root in young seedlings (Müller et al., 1998), was considered one of the most suitable candidates to test the potential contribution of the root gravitropic response to hook formation. Mature embryos of *pin2* mutants were dissected from seed coats and positioned either root-downwards or root-upwards to follow development of seedlings in real time. Hypocotyls of *pin2* mutants that germinated from the root-downwards orientation typically curved in alignment with the embryonic root and were mostly able to form an apical hook, although the maintenance phase of these hooks was shorter compared with wild-type seedlings (Col-0) (Fig. 2A,B, Movie 3). The root-upwards orientation severely interfered with hook curvature and the seedlings either randomly developed an apical hook, with significant delays, or in some individuals no apical hook formed (Fig. 2C,D, Movie 4). This difference in ability of *pin2* mutants to form an apical hook might correlate with penetrance of the root agravitropic phenotype, which we noticed was affected by initial orientation of mature embryos. In *pin2* mutants that started to germinate from a root-upwards orientation, root growth was more erratic compared with root-downwards positioned seedlings.

Recently, *NEGATIVE GRAVITROPIC RESPONSE OF ROOTS* (*NGR*)*/LAZY* genes were implicated in the direction of root

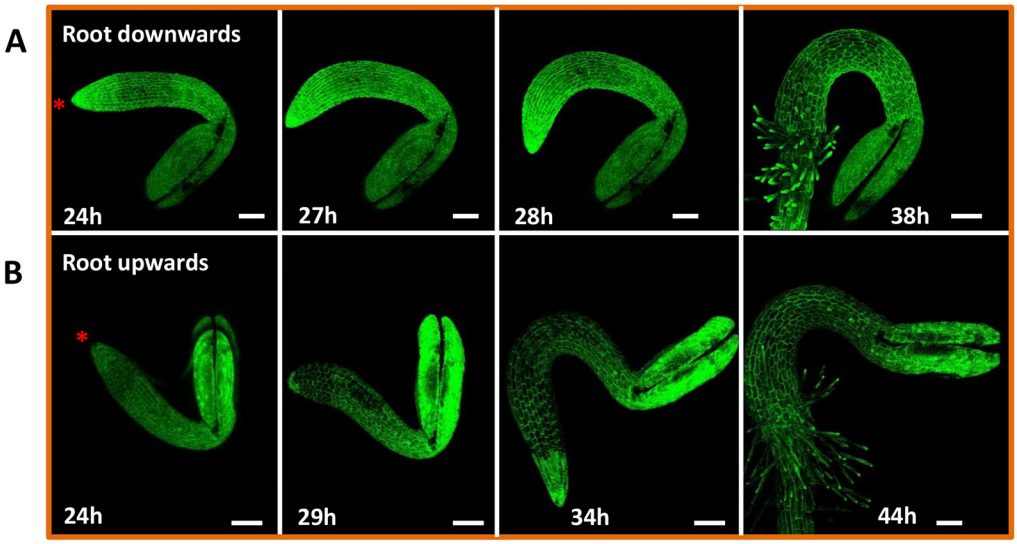

Fig. 1. Shape of mature embryo does not pre-determine formation of the apical hook. (A,B) The apical hook of seedlings developing from embryos oriented in either a root downwards (A) or upwards (B) position is formed in alignment with root gravity-triggered bending. h, time in hours after transfer for incubation. Asterisks indicate the root pole. Scale bars: 100 µm.

Development (2019) 146, dev175919. doi:10.1242/dev.175919

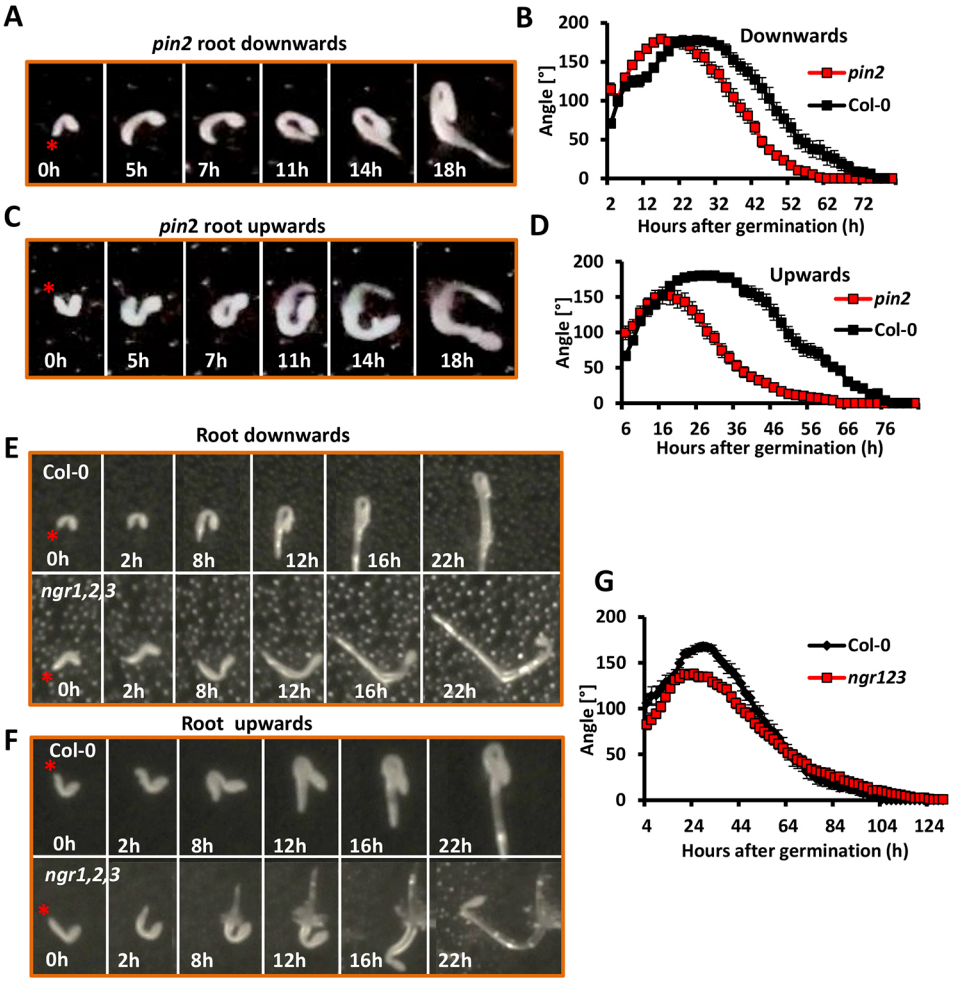

Fig. 2. Mutants impaired in the root response to gravity exhibit altered hook formation. (A-D) Real-time monitoring of apical hook formation in *pin2* seedlings developing from mature embryos positioned in root downwards (A,B) and upwards (C,D) orientations. h, time in hours after germination. (B,D) Quantification of the kinetics of apical hook development was carried out as described by Žádníková et al., 2010. For embryos facing downwards, Col-0 *n*=10 and *pin2 n*=11; for embryos facing upwards, Col-0 *n*=15, *pin2 n*=13. The experiment was repeated three times with similar results. (E-G) Real-time monitoring of apical hook formation in *ngr1,2,3* seedlings developing from mature embryos positioned in root downwards (E) and upwards (F) orientations. h, time in hours after germination. (G) Quantification of the kinetics of apical hook development. Col-0 *n*=23 and *ngr1,2,3 n*=22. The experiment was repeated three times with similar results. In images, asterisks indicate the root pole. In graphs, squares represent the average and error bars the s.e.m.

gravitropism. Unlike the agravitropic *pin2* mutant, in which a root growth defect is caused by insufficient basipetal (shoot-ward) auxin transport, roots of the *ngr1,2,3* triple mutant exhibit a negative gravitropic response. In the *ngr1,2,3* mutant, auxin accumulates at the non-stimulated side of root and, accordingly, it enhances root bending away from the gravity stimulus (Ge and Chen, 2016). Hence, the *ngr1,2,3* mutant was a suitable candidate for testing the correlation between root bending and apical hook formation. Monitoring mutant seedlings as they developed from the root-down or root-up orientated embryos revealed that the apical hook is formed in strict alignment with root bending (Fig. 2E-G). Remarkably, when the root of *ngr1,2,3* mutants is facing upwards, the hook is formed in a unique upside-down direction, opposed to the gravity stimulus, similar to observations of root growth (Fig. 2F). These results indicate that root bending is an essential cue that coordinates formation of the apical hook.

Interestingly, *root meristemless1* (*rml1*) mutants, despite a severe malfunction of the root apical meristem, as manifested by root growth arrest (Cheng et al., 1995), were still able to form apical hooks (Movie 5). Careful examination of the early phases of *rml1* seedling germination revealed that the embryonic root is able to grow and respond to the gravity stimulus, and that root growth arrest occurs only in the later phases of germination (Movie 5). Similarly, inhibition of the root gravity response as a consequence of lateral root cap-specific accumulation of AXR3, an auxin signaling repressor (Ouellet et al., 2001; Swarup et al., 2005), did not affect apical hook formation in either the root-down (Movie 6) or root-up (Movie 7) position. Detailed examination of *J0951*, an activator used specifically to stimulate *AXR3* in root tissues, revealed that its expression started only later, after the embryonic root outgrowth (Fig. S1E). Hence, in the early phase of germination, the embryonic root grew and responded to the gravity stimulus comparably to the wild-type control and loss of root gravitropism triggered by accumulation of AXR3 during later phases no longer interfered with formation of the apical hook.

The impact of early root gravity response deficiency on apical hook formation in *pin2* and *ngr1,2,3* mutants compared with *rml1* and *axr3* mutants indicates that there might be a short developmental window during which gravity-driven root bending acts as an important cue to coordinate formation of the apical hook. To assess the robustness and duration of such a developmental window, we turned seedlings 180° at different time points during germination and monitored the impact of the changed gravity vector on formation of the apical hook.

When embryos were turned shortly before or up to ∼6 h after germination started by root outgrowth, the apical hook always formed in alignment with the root bend (Fig. S2A,B, upper panel). However, changing the gravity vector at later time points (∼7-8 h after germination) by turning seedlings with emerged roots (longer than 0.7 mm) did not interfere with apical hook formation. Despite realignment of root growth due to gravistimulation, formation of the apical hook proceeded according to the original orientation determined by the root bend prior to turning (Fig. S2A,B, lower panel).

Development (2019) 146, dev175919. doi:10.1242/dev.175919

SCARECROW is an important regulator of endodermis formation, a layer that is essential for shoot gravitropism (Fukaki et al., 1998). To explore whether hypocotyl gravity response contributes to apical hook formation in addition to gravity-driven root bending, we examined *scr-3* mutants. We found that regardless of embryo orientation, *scr-3* seedlings were able to form the apical hook (Fig. S2C,D), suggesting that the hypocotyl gravity response might not be a limiting factor during apical hook formation.

Altogether, our results indicate that there is a short developmental window (less than 8 h after germination starts) during early phases of germination when the gravity-driven root bending acts as an important cue to trigger apical hook formation.

Light does not prevent apical hook formation driven by the root gravity response

It is accepted that the apical hook in dicotyledonous plants is generated when seedlings germinate in darkness, whereas light stimulates rapid opening of the apical hook (MacDonald et al., 1983; Raz and Ecker, 1999; Raz and Koornneef, 2001; Vandenbussche et al., 2010; Žádníková et al., 2010). Identification of the root gravity response as a light-independent cue that orchestrates the early phase of apical hook formation prompted us to hypothesize that the apical hook might be formed irrespective of light conditions. To test this hypothesis, we germinated seedlings under constant illumination. Real-time monitoring revealed that early phases of seedling development in light resemble those occurring in darkness and light does not prevent formation of the apical hook curvature. As seedlings start to grow, the embryonic root rapidly expands, bends downwards with the gravity vector and drives formation of the apical hook (Fig. 3A, Movies 8,9). However, unlike etiolated seedlings, the apical hook formed in constant light exhibits a very short maintenance phase and tends to rapidly open (Fig. 3B). In summary, these results support the hypothesis that gravity-stimulated root bending is a crucial factor that coordinates apical hook formation regardless of light conditions.

Establishment of an auxin maximum during early phases of apical hook formation

Apical hook formation is driven by auxin, local accumulation of which in epidermal cells at one side of hypocotyl defines the concave side of the hook curvature (Raz and Ecker, 1999). Although functional polar auxin transport has been implicated in establishment of the auxin maximum, the mechanisms that govern the asymmetry of auxin distribution are unknown. To explore how and when the auxin maximum that drives formation of the apical hook is established during germination, mature embryos dissected from their seed coats were grown on the Murashige and Skoog (MS) medium and expression of *DR5*-derived auxin response reporters was carefully monitored during germination. As expected, mature embryos exhibited auxin response maxima in cotyledons and root columella cells; however, no *DR5* activity in embryonic hypocotyls prior germination could be detected (Fig. 4A, Fig. S3A,B). Typically, germination of seedlings starts by expansion of the embryonic root and rapid adjustment of its growth direction with the gravity vector. The gravitropic response of the root is coordinated by asymmetric auxin distribution (Ottenschlager et al., 2003; Kleine-Vehn et al., 2010) and, accordingly, we observed a higher auxin signal at the lower (gravity-stimulated) side of the growing root (Fig. 4A, Fig. S3A,B). Over time, a transient auxin response maximum appeared at the root-hypocotyl junction and this local accumulation of hormone correlated with a local bending, which can be considered as the start of apical hook formation (Fig. 4A, Fig. S3A,B). At around 36 h, the local auxin maximum at the root-hypocotyl junction fades, but as the hypocotyl continues to grow, the auxin response at the concave side of the hook region becomes gradually stronger and the hook continues to bend until it is fully closed (Fig. 4A, Fig. S3B). A similar pattern of auxin response maximum establishment was observed using *DR5::RFP* reporter in seedlings germinated in light (Fig. S3C).

Hence, during seedling germination the earliest detectable asymmetry in auxin distribution is linked with the root response

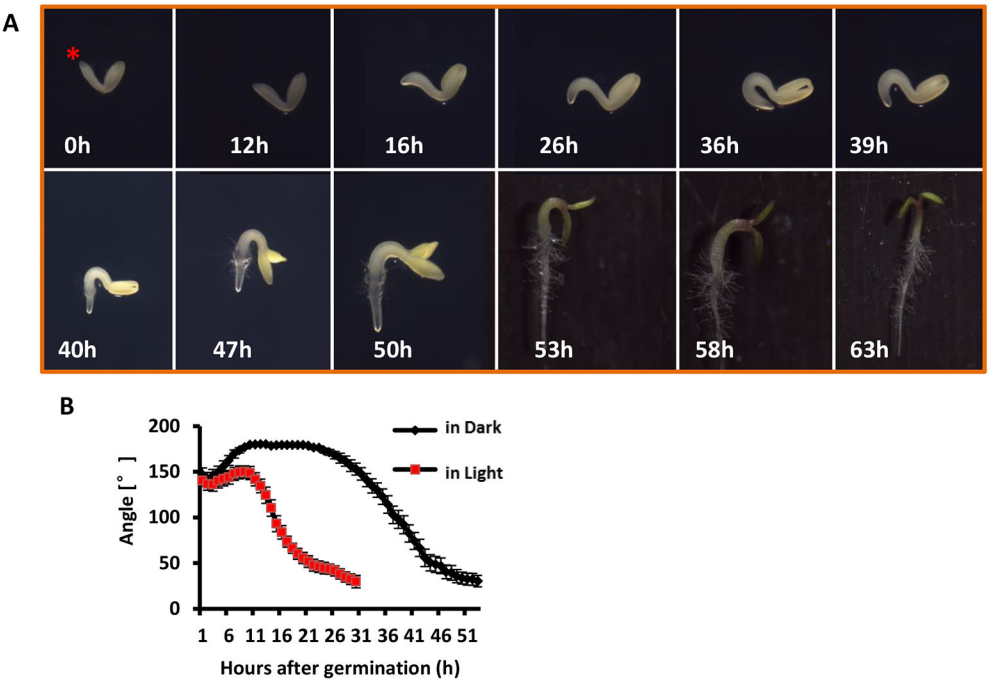

Fig. 3. Root gravitropic response directs apical hook formation regardless of illumination. (A,B) Real-time monitoring of apical hook formation in seedlings developing from embryos positioned root-downwards under constant illumination (A) and kinetics of the apical development in seedlings growing in light versus dark (B). h, time in hours after transfer for incubation (A) and after germination (B). Asterisk indicates a root pole. Squares represent the average and error bars the s.e.m. Light n=10, dark n=15. The experiment was repeated three times with similar results.

Development (2019) 146, dev175919. doi:10.1242/dev.175919

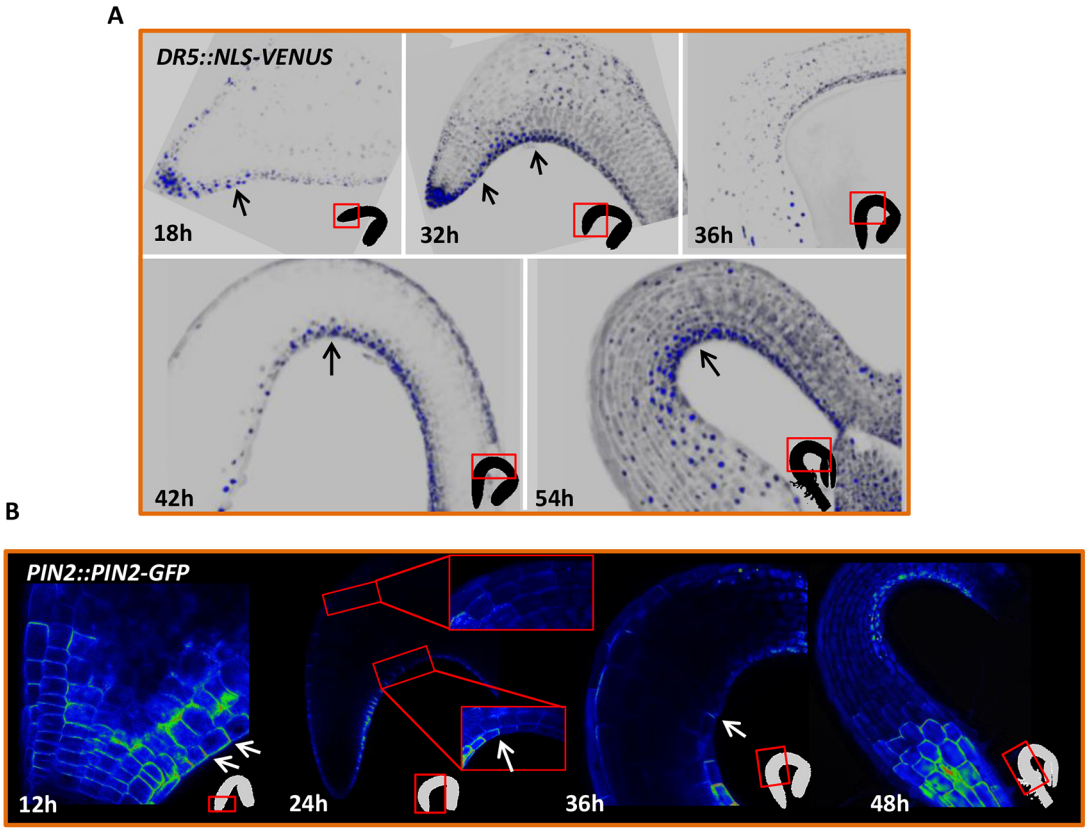

Fig. 4. Root response to gravity triggers asymmetry in auxin distribution during early phases of germination. (A) Monitoring of *DR5::NLS-VENUS* auxin reporter expression during germination. Reporter signal in the nucleus (blue) is at first detected at the gravi-stimulated side of root (18 h); at 32 h, auxin response maximum is detected at the root-hypocotyl junction; from 42 h on, auxin response at the concave side of the apical hook is detected. h, time in hours after transfer for incubation. Black arrows indicate auxin response maximum. (B) Monitoring of *PIN2::PIN2-GFP* during apical hook formation. At 12 h, PIN2-GFP is detected at the apical plasma membranes of root epidermal cells (white arrows). Higher expression is observed at the gravi-stimulated side of the root. From 24 to 48 h, PIN2-GFP is detected at the root-hypocotyl junction extending to hypocotyl epidermal cells (white arrows). Insets indicate developmental stage of seedlings with red rectangle marking the magnified zone. h, time in hours after transfer for incubation.

to gravity stimulus and afterwards a local auxin maximum that correlates with the formation of hook curvature is observed.

Polar auxin transport machinery mediating root gravitropic bending is established during the early phases of germination

Root gravitropic bending as well as apical hook formation are driven by asymmetric auxin distribution mediated by polar auxin transport machinery with PIN2, PIN3, PIN4 and PIN7 being major efflux carriers involved in both these processes (Kleine-Vehn et al., 2008; Abbas et al., 2013; Žádníková et al., 2016). Typically, *PIN2* expression is restricted to the root meristem where its localization at the apical membranes of epidermal cells mediates the basipetal (shoot-ward) auxin transport required for the proper root gravity response (Müller et al., 1998; Kleine-Vehn et al., 2008). Interestingly, during the early phases of germination the boundary between the root and the hypocotyl seems to be not strictly defined and PIN2 was detected in hypocotyls where it localizes to the apical membranes of epidermal cells (Fig. 4B, Fig. S5A). As the hypocotyl and root expanded, *PIN2* expression in hypocotyls ceased, and remained restricted to the root meristem, as previously reported (Müller et al., 1998). The lack of a precisely confined border of *PIN2* expression at the root-hypocotyl junction indicates that, at early phases of seedling germination, PIN2 might transport auxin across the root zone towards the hypocotyl. Also, early expression of *PIN3* and *PIN7* was detected in the root columella cells where they can contribute to the perception of gravity stimulus (Figs S4A,B, S5B-D; Friml, 2003; Kleine-Vehn et al., 2010). In embryonic hypocotyls, the expression of PIN genes is generally low, and as seedlings germinate and the apical hook gradually forms, it progressively enhances (Figs S4A,B, S5B-D; Žádníková et al., 2010). Similar patterns of PIN gene expression were detected in germinating seedlings exposed to light (Fig. S6A-D). Altogether, the spatiotemporal pattern of PIN gene expression indicates that the transport machinery, which mediates auxin redistribution to coordinate the root gravitropic response, is established at very early phases of germination, and subsequently the transport system for auxin redistribution through the hypocotyl is formed.

Seedlings germinated from embryos before de-greening exhibit a normal root gravity response, but do not form an apical hook

Our results indicate that root gravitropic bending acts as an important regulatory cue for apical hook formation and that the apical hook can be formed under both dark and light conditions. Hence, we hypothesized that, rather than light conditions, a predetermination of the skoto-morphogenic developmental program in seedlings germinating from mature non-green embryos might be decisive for apical hook formation. To test this hypothesis, we examined seedlings developing from mature embryos prior to

Development (2019) 146, dev175919. doi:10.1242/dev.175919

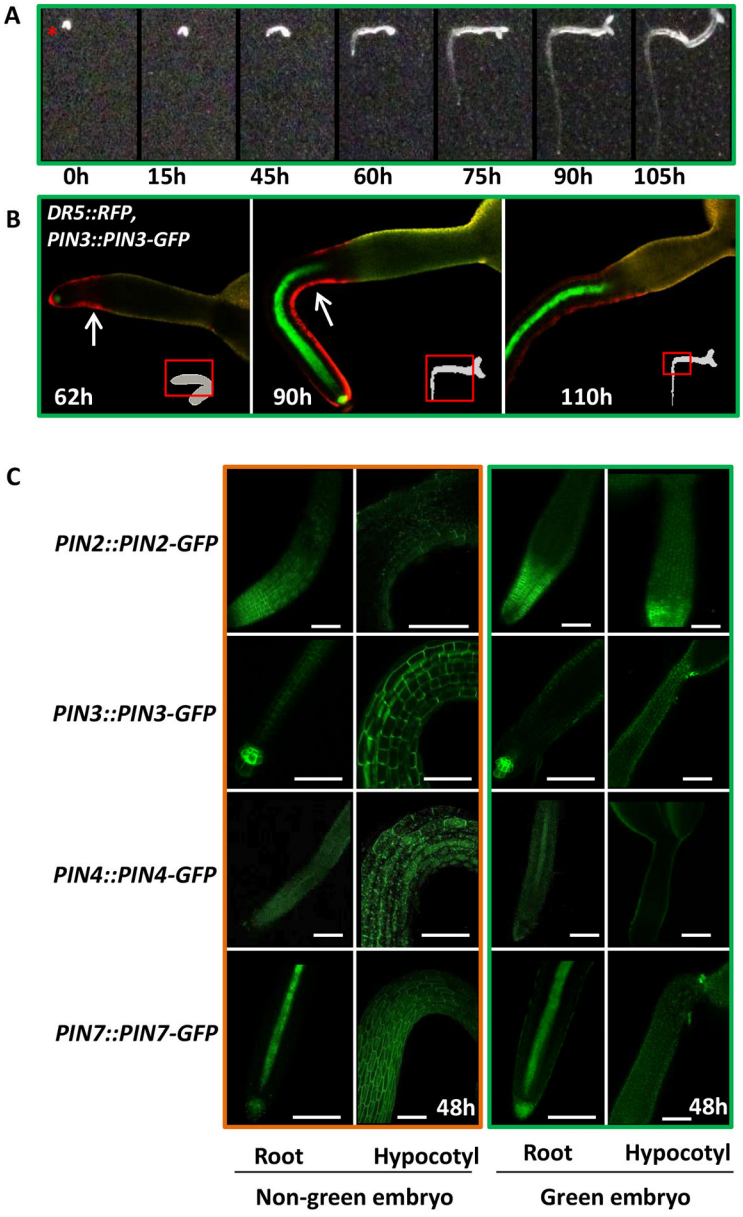

Fig. 5. Seedlings germinated from green embryos do not form the apical hook. (A) Real-time monitoring of seedlings developing from green embryos in the darkness. No apical hook formation is observed. h, time in hours after start of germination. Asterisk indicates the root pole. (B) Monitoring of *DR5::RFP* auxin reporter expression during germination of seedlings from green embryos. Reporter red signal is first detected in the gravi-stimulated side of root (62 h); at 90 h, auxin response maximum is detected at the root-hypocotyl junction, but no auxin response maxima in the hypocotyl is detected at any time point. Green signal corresponds to *PIN3::PIN3-GFP* marker line, which shows normal expression in roots, but no specific signal in shoot. h, time in hours after transfer for incubation. White arrows indicate auxin response maximum in root. Insets indicate developmental stage of seedlings with red rectangle marking the magnified zone. (C) Expression of *PIN2::PIN2-GFP*, *PIN3::PIN3-GFP*, *PIN4::PIN4-GFP* and *PIN7::PIN7-GFP* in root and hypocotyls (focused at the apical hook zone) of seedlings developing from either non-green or green embryos. h, time in hours after transfer for incubation. Scale bars: 100 µm.

de-greening (normally around 12-14 days after fertilization; Delmas et al., 2013). When monitored in real time, we found that seedlings developing from green embryos initiate germination by outgrowth of the embryonic root and its proper alignment with the gravity vector; however, hypocotyls of such seedlings are not able to form an apical hook (Fig. 5A, Movies 10,11). Importantly, seedlings developing from green embryos are fully viable and after 10 days largely comparable to those grown from non-green embryos under the light (Fig. S7). Hence, although seedling roots from germinating green embryos respond properly to gravity, this early stimulus is not transmitted into the differential hypocotyl growth required for apical hook formation. Because asymmetric redistribution of auxin directs both root gravitropic bending and apical hook formation, we monitored the auxin response in seedlings germinating from green embryos. Similarly to non-green embryo seedlings, those germinating from green embryos exhibited asymmetric auxin distribution that correlates with the root gravity response. However, no auxin asymmetry and formation of local maxima could be detected in hypocotyls of such seedlings (Fig. 5B). Together, these results indicate that apical hook formation might be dependent on two mechanisms, root gravity perception and hypocotyl-specific regulatory machineries, that control auxin distribution in a coordinated way.

Polar auxin transport machineries in seedlings germinated from green versus non-green embryos are established differently

A complete lack of the auxin response maximum and hook formation in seedlings germinated from green embryos, despite their normal root gravity response, provided a valuable model to further explore requirements for establishment of the polar auxin transport that guides bending of the hook. Detailed analysis of the spatiotemporal expression patterns in early phases of development revealed that *PIN2* and *PIN4* in seedlings germinating from green embryos are, apart from roots, also expressed in hypocotyls (Fig. S8A,B). Both *PIN3* and *PIN7* were expressed in seedlings

Development (2019) 146, dev175919. doi:10.1242/dev.175919

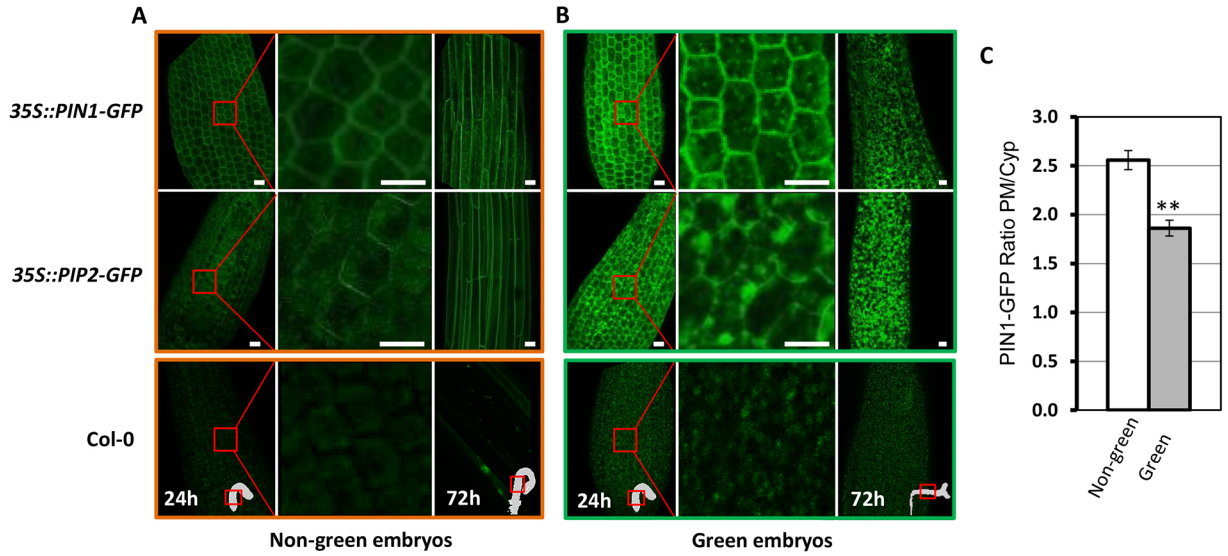

Fig. 6. Trafficking of PINs to the plasma membrane is affected in hypocotyls germinated from green embryos. (A,B) Subcellular localization of PIN1-GFP and PIP2-GFP in the epidermal hypocotyl cells of seedlings germinated from non-green (A) and green (B) embryos. Insets indicate developmental stage of seedlings with red rectangle marking the magnified zone. Col-0 was used as the wild-type control. h, time in hours after transfer for incubation. (C) Ratio of the plasma membrane (PM) to intracellular cytosolic (Cyp) PIN1-GFP signal in hypocotyl epidermal cells of seedlings grown for 24 h from either non-green or green embryos of *35S::PIN1-GFP*. Bars represent the average and error bars the s.e.m. ***P*<0.01. *n*=22 cells from 3 different embryos. Scale bars: 20 µm.

germinated from green embryos from 24 h onwards. Their expression was confined to the central vasculature of hypocotyls and a weaker signal in outer tissues, including cortex and epidermis, could be detected (Fig. S8A,B). Quantitative RT-qPCR analysis largely corroborated these results (Fig. S8E). Surprisingly, despite detectable transcription of PIN genes, no PIN proteins were found in hypocotyls of seedlings developing from green embryos, either by observation of PIN-GFP lines using confocal microscopy (Fig. 5C), or by western blot analysis applying antibodies specific to GFP (Fig. S8F). In roots, regardless of whether grown from green or non-green embryos, membrane localized PINs were detected exhibiting expression patterns as previously described (Fig. 5C, Müller et al., 1998; Friml, 2003; Blilou et al., 2005). Together, these results indicate a notable difference in establishment of the auxin transport system in seedlings germinated from non-green versus green embryos. Whereas seedlings developing from non-green embryos establish auxin transport in both roots and hypocotyls, PIN-mediated transport in hypocotyls of seedlings originating from green embryos is largely attenuated.

Trafficking of PINs to the plasma membrane is affected in hypocotyls germinated from green embryos

The lack of PINs in hypocotyls grown from green embryos prompted us to test whether enhancement of PIN expression might be sufficient to recover the auxin transport required for apical hook formation. Constitutive *35S* promoter-driven expression of *PIN1-GFP* was unable to promote hypocotyl growth and formation of the apical hook in seedlings germinated from green embryos (Fig. S9A). Detailed observation of subcellular localization revealed that weak or no membrane-localized PIN1-GFP signal could be detected in hypocotyls grown from green embryos; instead, a high accumulation in intracellular bodies was found. As expected in hypocotyls developing from non-green embryos, membrane-localized PIN1-GFP was observed with no (or very small) intracellular bodies. Those effects were clearer at 72 h, but could be seen at times as early as 24 h after germination (Fig. 6). In roots, PIN1-GFP was located in the plasma membrane regardless of whether grown from green or non-green embryos (Fig. S9B). Similarly to PIN1, the aquaporin PLASMA MEMBRANE LOCALIZED PROTEIN2 (PIP2; Dhonukshe et al., 2007) accumulated within hypocotyl cells with weak or no signal in the plasma membranes (Fig. 6), although in roots its plasma membrane localization was clearly detected (Fig. S9B). This suggests that subcellular trafficking of membrane proteins in hypocotyls of seedlings developing from green embryos dramatically differs from that occurring in hypocotyl cells of seedlings originating from non-green embryos.

ABA prevents establishment of the hypocotyl auxin transport system required for apical hook formation

Maturation of green embryos and their de-greening have been shown to be under negative control of the plant hormone abscisic acid (ABA). Typically, green embryos exhibit a peak of ABA concentration that decreases during the de-greening process (Nambara et al., 1995; Delmas et al., 2013). Consistent with this, we detected a higher expression of genes involved in ABA synthesis and signaling, as well as a downregulation of genes involved in ABA inactivation, in seedlings developing from green versus non-green embryos (Fig. S10A). To test whether a higher level of ABA might underlie the differences in hypocotyl growth and the lack of apical hook in seedlings developing from green compared with non-green embryos, we examined seedlings grown from non-green embryos in the presence of ABA. We found that ABA treatment severely restricted hypocotyl growth and the formation of the apical hook, but it did not prevent embryonic root outgrowth and its gravity response, thus strongly mimicking the phenotype of seedlings germinated from green embryos (Fig. 7A compared with 5A). Also, the effect of ABA on PIN gene expression largely resembled the pattern observed in seedlings developed from green embryos (Fig. S8C-E). Similar to observations in hypocotyls developed from green embryos, ABA enhanced expression of *PIN2* and *PIN4*,

Development (2019) 146, dev175919. doi:10.1242/dev.175919

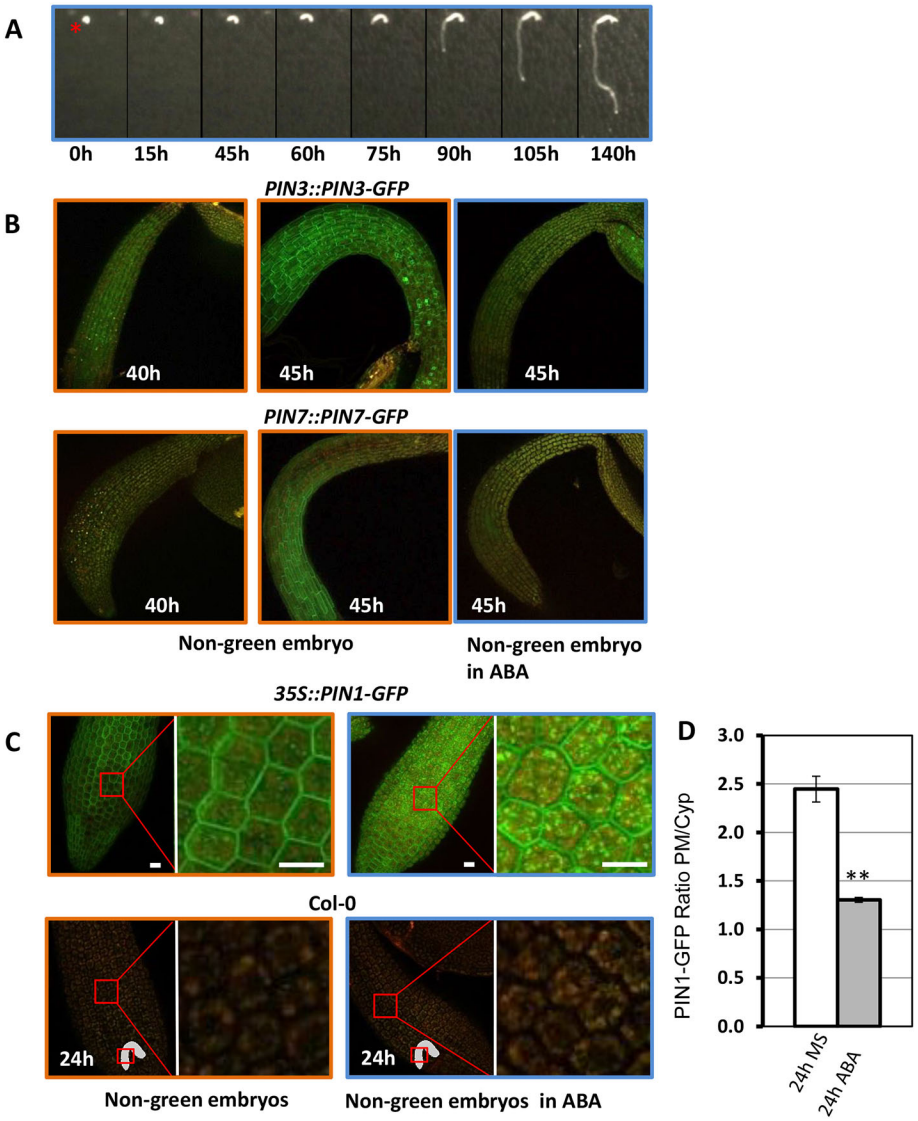

Fig. 7. ABA blocks apical hook formation and interferes with PIN trafficking to the plasma membrane of hypocotyl cells. (A) Real-time monitoring of seedlings developing from non-green embryos treated with 0.1 µM ABA in the darkness. h, time in hours after transfer for incubation. Asterisk indicates the root pole. (B) Membrane localization of PIN3-GFP and PIN7-GFP is compromised in seedlings germinated from non-green embryos exposed to 10 µM ABA for 5 h. (C) ABA treatment (10 µM ABA in MS for 24 h) of seedlings germinating from non-green embryos interferes with targeting of PIN1 to the plasma membrane of hypocotyl epidermal cells. (D) Ratio of the plasma membrane (PM) to intracellular cytosolic (Cyp) PIN1-GFP signal in hypocotyl epidermal cells of seedlings either on MS or after ABA treatment. h, time in hours after transfer for incubation. Insets indicate developmental stage of seedlings with red rectangle marking the magnified zone. Bars represent the average and error bars the s.e.m. $^{**}P<0.01$. $n=20$ cells from 3 different embryos. Scale bars: 20 µm.

whereas *PIN3* and *PIN7* expression was largely restricted to the central cylinder (Fig. S8C). Moreover, the inhibitory effect of ABA on hypocotyl growth and PIN gene expression could be eliminated by washing out the hormone (Fig. S8D). Also, as in seedlings developing from green embryos, an auxin maxima could not be detected in hypocotyls of ABA-treated non-green seedlings (Fig. S10B). Next, we tested whether ABA interferes with trafficking of plasma membrane proteins as observed in hypocotyls germinated from green embryos. Whereas membrane-localized PIN3 and PIN7 were observed in untreated hypocotyls, in the presence of ABA (5 h) no membrane-localized PINs in hypocotyl cells could be detected, although expression in this organ was still detectable (Fig. 7B, Fig. S10C). These results suggest that ABA might interfere with the proper trafficking of PINs to the plasma membrane of hypocotyl cells. To examine further the ABA effect on membrane protein trafficking, seedlings constitutively expressing *PIN1* under the *35S* promoter were treated with ABA. ABA enhanced intracellular accumulation of PIN1 in epidermal cells of hypocotyls compared with untreated control (Fig. 7C,D). Hence, similarly to green embryos, ABA interfered with the proper establishment of the auxin transport system required for apical hook formation in hypocotyls.

A tight ABA-GA balance is required to coordinate hypocotyl growth and hook formation

High ABA activity was identified as a potential factor that might interfere with establishment of the auxin transport machinery required for apical hook formation in hypocotyls of seedlings germinated from green embryos. To test whether reduction of ABA levels during germination of seedlings from green embryos might lead to a recovery of apical hook formation, we applied chemical and genetic tools. Reduction of ABA levels either chemically, using a synthetic inhibitor of ABA biosynthesis abamine (Abm; Han et al., 2004), or genetically, in a mutant defective in ABA biosynthesis, *Arabidopsis thaliana aba deficient 2* (*aba2*; Nambara et al., 1998) (*ABA2* is highly expressed in green embryos; Fig. S10A), did not lead to recovery of apical hook formation. Similar to untreated seedlings germinating from green embryos, the growth and gravity response of Abm-treated wild-type Col-0 and *aba2* roots were largely unaffected, whereas the hypocotyls of both Abm-treated Col-0 as well as *aba2* seedlings were unable to undergo elongation and form apical hooks (Fig. 8A,C). Moreover, additional reduction of ABA levels by applying Abm to the *aba2* mutant also did not result in recovery of apical hook formation (Fig. 8D, Table S1). This indicated that reduction of ABA alone is not sufficient to promote apical hook formation and another

Development (2019) 146, dev175919. doi:10.1242/dev.175919

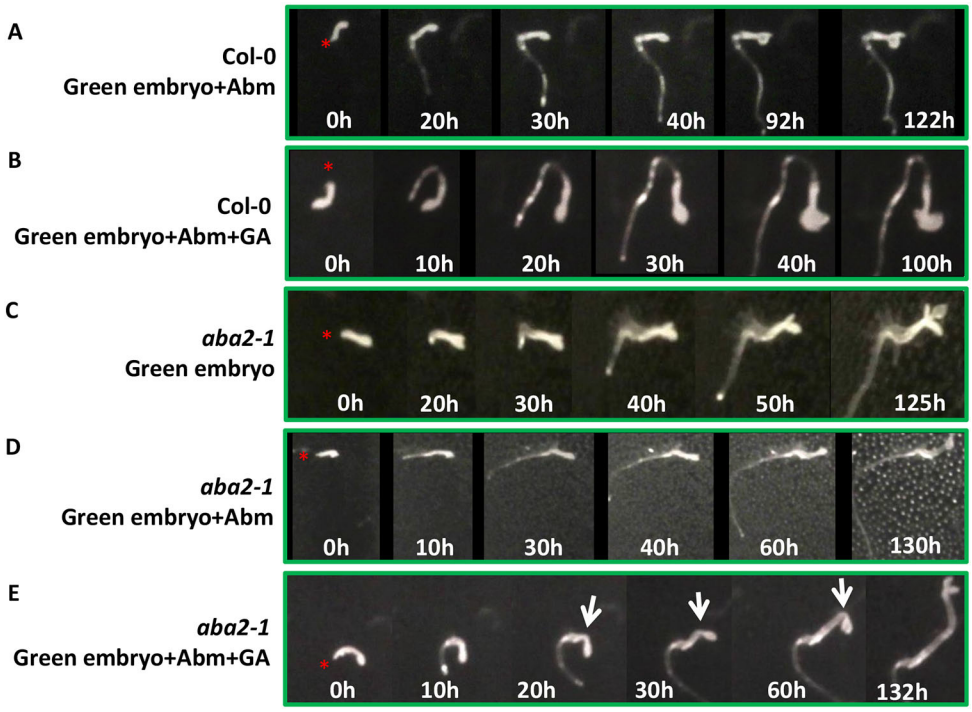

Fig. 8. Reduction of ABA and increase of GA3 recover the apical hook formation in seedlings developing from green embryos. (A-E) Real-time monitoring of seedlings developing from green embryos of wild-type Col-0 (A,B) and *aba2-1* mutant (C-E) in the presence of the ABA biosynthesis inhibitor abamine (Abm; 100 µM in MS) (A,D); or Abm and gibberellin (GA; 50 µM GA3 in MS) (B,E). h, time in hours after germination. Asterisks indicate the root pole, white arrows point to the forming apical hook.

regulatory factor might be involved. Seed maturation and germination are two tightly linked processes antagonistically regulated by ABA and GAs (Stamm et al., 2017; Liu and Hou, 2018). However, application of GA3 was not sufficient to promote hypocotyl elongation growth and hook formation in seedlings germinating from green embryos in the presence of Abm (Fig. 8B). Only when levels of ABA were reduced by applying Abm to *aba2* and GA3 levels were increased simultaneously were both the hypocotyl growth and the apical hook formation recovered (Fig. 8E, Table S1). Together, these results suggest that, during embryo maturation and the transition to germination, a tight ABA-GA balance is required to stimulate hypocotyl growth and apical hook formation.

DISCUSSION

Apical hook formation is a result of differential growth, with auxin being a key player to guide asymmetry of cell elongation at the concave versus convex side of the hypocotyl (Raz and Ecker, 1999). Intriguingly, no asymmetry in auxin distribution and expression of PINs could be detected in embryonic hypocotyls prior to seedlings starting to develop, thus raising a question about the regulatory factors that determine the local increase of auxin that drives formation of the apical hook.

Thorough monitoring of auxin responses identified the gravi-stimulation of embryonic roots as one of the earliest triggers of asymmetric auxin distribution after seedlings start to germinate. This growth response, underpinned by redistribution of auxin towards the gravi-stimulated side of the root (Ottenschlager et al., 2003; Kleine-Vehn et al., 2010), is particularly important at early phases of germination when emerging roots adjust their growth direction with the gravity vector. Our work suggests that this gravity-driven root bending acts simultaneously as an important regulatory cue for apical hook formation. Real-time monitoring of seedlings germinating from embryos positioned either in a root downwards or upwards orientation showed that apical hooks are formed in a strict alignment with root bending. In contrast, the curved shape of mature embryos enclosed in the seed coat does not necessarily pre-determine a hook bend and can be overridden by gravity-driven root bending. Lack of the root gravity response in either the *pin2* mutant or after mechanical destruction of the root tip interferes with apical hook formation. Observation of the *ngr1,2,3* mutant further supports a contribution of the root bending as an initial cue in apical hook formation. Despite the fact that this negatively gravitropic mutant has roots that bend away from the gravity vector, the apical hook still aligns with the curvature of the root. Importantly, as in wild type, root bending is driven by auxin. Although in *ngr1,2,3* mutants its increase at the non-gravi-stimulated side promotes bending away from the gravity vector (Ge and Chen, 2016; Yoshihara and Spalding, 2017). The ability to form a hook is maintained in seedlings germinating under constant light, an established trigger of hook opening, thus further supporting a dominating role of root bending in initial phases of apical hook formation. On the other hand, interference with root growth and gravity response during later germination phases does not affect formation of the apical hook, suggesting that there is a short developmental window after germination starts when root bending coordinates formation of the hook curvature. Perturbation of the gravity vector during development by rotating seedlings indicates that the developmental window critical for determination of the apical hook is ∼8 h from the start of germination. Altogether, these results support a model in which, during early phases of germination, a gravity-stimulated asymmetry in auxin distribution coordinates root bending and, consequently, the formation of the apical hook. However, *scr-3* mutants affected in hypocotyl gravitropism did not exhibit any dramatic defects in the formation of the apical hook, indicating that hypocotyl response to gravity might not be limiting for formation of the hook.

It is worth noting that studies examining plant growth in microgravity conditions reported that apical hooks may be formed even under zero gravity (Ueda et al., 2000; Miyamoto et al., 2014). In agreement with these reports, our results (in particular the observations in *ngr1,2,3* mutants) suggest that root bending, rather than gravi-stimulus per se, directs formation of the hook. Hence, in

Development (2019) 146, dev175919. doi:10.1242/dev.175919

zero gravity, any bending of the root, which could be potentially triggered by other stimuli (e.g. negative root phototropism), might lead to the apical hook formation.

Over recent years, the mechanism controlling auxin redistribution in gravi-stimulated roots has been uncovered (Bennett et al., 1996; Galweiler et al., 1998; Luschnig et al., 1998; Müller et al., 1998; Friml et al., 2002; Swarup et al., 2005; Harrison and Masson, 2008). In response to gravity, PIN3 and PIN7 rapidly relocate from apolar to polar membrane localization with maxima at the bottom of root columella cells, which leads to an increase of auxin transported via PIN2 at the lower side of the gravi-stimulated root (Friml et al., 2002; Kleine-Vehn et al., 2010). Higher auxin limits cell expansion and ultimately promotes root bending (Ottenschlager et al., 2003; Brunoud et al., 2012). In line with a proposed role of the root gravity-stimulated bending as an initial factor coordinating apical hook formation, early onset of *PIN3*, *PIN7* and *PIN2* expression in root columella and epidermal cells was observed.

However, the question remains of how this initial stimulus related to the auxin-driven root bending is transmitted to coordinate formation of the apical hook. Detailed monitoring of PIN2 indicates that during early phases of germination, expression of this efflux carrier is not restricted to the root, but it extends towards a hypocotyl. Thus, PIN2-mediated polar auxin transport might contribute to the initial accumulation of auxin at (above) a root-hypocotyl junction and thereby stimulate differential growth of cells in this zone. In the hypocotyls, this initial auxin-driven growth asymmetry might be further reinforced by gradually established auxin transport machinery. Accordingly, we found that prior to germination the expression of *PIN* homologs, including *PIN3*, *PIN4* and *PIN7*, in embryonic hypocotyls is low and that progressively, as seedlings grow, it gradually increases, adopting the pattern reported previously (Žádníková et al., 2010, 2016).

Another intriguing aspect is the establishment of axial asymmetry of PINs that reinforces an auxin response maximum formed initially because of root response to gravity mediated by PIN2. We propose that the initial auxin-driven differential growth at the root-hypocotyl junction might lead to the formation of a regulatory feedback loop, which reinforces an asymmetry in PIN expression and subcellular dynamics in cells at the outer versus inner side of bending hypocotyls. An important part of this regulatory feedback loop might be growth-related differences in mechanical forces in cells at the outer and inner side of the bending hypocotyl. Changes in mechanical strains, such as modifications of turgor pressure or the application of external force, have been found to affect subcellular trafficking and membrane localization of PINs. In tissue under strain, a higher proportion of PIN localized to the plasma membrane has been detected (Nakayama et al., 2012). Additionally, a differential distribution of auxin needs to be considered as an important element of this regulatory feedback loop. Auxin has been found to promote expression of *PIN3* and *PIN4*, to attenuate *PIN7* transcription, and to inhibit endocytosis of PINs. Thus, auxin might be an important factor in the establishment and maintenance of axial asymmetry of PINs in the hypocotyl (Paciorek et al., 2005; Vieten et al., 2005; Uyttewaal et al., 2010, 2012; Peaucelle et al., 2011).

The phenotype of seedlings germinating from green embryos hinted at additional aspects of mechanisms underlying the apical hook formation. First, the importance of proper root-hypocotyl communication via two tightly coordinated auxin transport machineries and, second, the role of the ABA pathway to preset mature embryos for the establishment of the polar transport machinery anew. We found that, unlike seedlings germinated from mature non-green embryos, hypocotyls of seedlings developing from mature, but still green embryos were not able to perceive and transmit the root-bending stimulus towards apical hook formation. Detailed observations of auxin and polar auxin transport machinery revealed that whereas in seedlings originating from non-green embryos the establishment of the polar auxin transport machinery in roots and hypocotyls was tightly co-regulated, in hypocotyls developing from green embryos PIN-mediated transport was significantly suppressed. These data indicate that formation of the apical hook is dependent on the coordinated establishment of polar auxin transport machineries in both roots and hypocotyls.

Mature embryos prior to de-greening are under strong control of ABA (Frey et al., 2004; Finch-Savage and Leubner-Metzger, 2006), as corroborated by the expression analysis of several ABA regulatory network components. Interestingly, seedlings developing from non-green embryos in the presence of ABA resemble those germinated from green embryos. Similar to seedlings developing from green embryos, hypocotyl growth and formation of the apical hook were severely suppressed by ABA applied to non-green embryos. This deficiency in hypocotyl growth and apical hook formation correlate with attenuated expression and trafficking of PINs to the plasma membrane. It is worth noting that similar effects of ABA on PIN expression have been reported in roots (Shkolnik-Inbar and Bar-Zvi, 2010; Yang et al., 2014; Rowe et al., 2016), although our results suggest that embryonic hypocotyls exhibit higher sensitivity to ABA compared with roots. Hence, high ABA in green embryos might be part of the regulatory pathway that at the end of embryogenesis helps to restrain former polar auxin transport machinery and thus enables to create a '*tabula rasa*' on which a novel auxin transport system can be established as seedlings start to germinate. Recovery of the apical hook formation in seedlings developing from green embryos after simultaneous reduction of ABA and increase of GAs further suggests that a tight balance between both hormones is required to guide hypocotyl growth and apical hook formation.

Based on our observations, we propose a model for the establishment of auxin transport that guides apical hook formation. High levels of ABA during maturation of embryos promote pathways that suppress expression of polar auxin transport components and erase remnants of PINs from the membrane. As a result, mature embryos, after de-greening, are deprived of former auxin distribution machineries, which enables them to build the auxin transport system anew. During germination initiated by outgrowth of roots and their alignment with the gravity vector, *PIN3*, *PIN7* in columella and *PIN2* in root epidermal cell are expressed first. Extended expression of *PIN2* towards the root-hypocotyl junction enables formation of a local auxin maximum at the transition zone, thereby triggering differential growth. The differential cell expansion at the root-hypocotyl junction driven by auxin might, together with GAs, lead to the establishment of a regulatory feedback loop reinforcing the differential expression and subcellular dynamics of PINs at the outer and inner sides of bending hypocotyls that are required for the auxin maxima and apical hook formation.

MATERIALS AND METHODS

Plant material

Arabidopsis thaliana (L.) Heynh (*Arabidopsis*) plants were grown in a growth chamber at 21°C under white light, which was provided by blue and red LEDs (70-100 µmol m^{-2} s^{-1} of photosynthetically active radiation). The transgenic lines used have been described elsewhere: *DR5::GUS* (Sabatini et al., 1999); *PIN1::GUS*, *PIN2::GUS*, *PIN3::GUS*, *PIN4::GUS*, *PIN1::PIN1-GFP* and *PIN7::PIN7-GUS* (Benková et al., 2003); *PIN7::GUS* and

Development (2019) 146, dev175919. doi:10.1242/dev.175919

PIN4::PIN4-GFP (Vieten et al., 2005); *PIN3::PIN3-GFP* and *PIN7::PIN7-GFP* (Žádníková et al., 2010); *pin2* mutant and *rml1* mutant (Cheng et al., 1995); J0951≫UAS-AXR3 (Swarup et al., 2005); *35S::PIN1-GFP* (Marhavý et al., 2011); *PIN2::PIN2-GFP* (Xu and Scheres, 2005); *35S::PIP2-GFP* (Cutler et al., 2000); *ngr1,2,3* (Ge and Chen, 2016); and *scr-3* and *aba2-1* from NASC.

Growth conditions

Seeds were sterilized in 5% bleach for 10 min and rinsed with sterile water before plating on half-strength MS medium (Duchefa) with 1% sucrose, 1% agar (pH 5.7). Seeds were stratified for 3-4 days at 4°C, exposed to light for 2-4 h at 21°C, and cultivated in the growth chamber under appropriate light conditions at 21°C (wrapped in aluminum foil and placed in a cardboard box for dark growth, or into light in the same chamber). For non-green embryos, seeds were dissected after stratification and imbibition in water. For green embryos, flowers were marked by a marker line on the stem or by tying small thread on it, and siliques around 12-14 days after fertilization were used for the dissection as described elsewhere (Delmas et al., 2013). Seedlings were processed at the indicated times after germination or used for real-time phenotype analysis. Real-time analysis and statistics of apical hook development of seedlings were recorded at 1 h intervals for 5 days at 21°C with an infrared light source (880 nm LED; Velleman, Belgium) or constant light by a spectrum-enhanced camera (EOS035 Canon Rebel Xti, 400DH) with built-in clear wideband-multicoated filter and standard accessories (Canon) and operated by EOS utility software as previously described (Zhu et al., 2017). Angles between the hypocotyl axis and cotyledons were measured using ImageJ (NIH; http://rsb.info.nih.gov/ij) as described previously (Žádníková et al., 2010). Fifteen to twenty seedlings were processed.

Chemicals used

Indole-3-acetic acid, 1-naphthaleneacetic acid (NAA) and abscisic acid (ABA) were from Sigma-Aldrich and were used as 10 mM in ethanol stocks. Gibberellic acid (GA3) (Sigma-Aldrich) was dissolved at 100 mM in ethanol. Abm was synthesized and purified as detailed in supplemental Materials and Methods and was dissolved at 10 mM in DMSO stock.

GUS analysis

Histochemical β-glucuronidase (GUS) staining was performed as described (Jefferson et al., 1987) with minor modifications. In brief, the GUS reaction was carried out in reaction buffer containing 0.1 M sodium phosphate buffer (pH 7), 1 mM ferricyanide, 1 mM ferrocyanide, 0.1% Triton X-100 and 1 $mgml^{-1}$ X-Gluc for overnight incubations at 37°C. The GUS reaction was stopped by washing in 70% ethanol, and clearing performed by incubation in a solution containing 4% HCl and 20% methanol for 15 min at 57°C, followed by 15 min incubation in 7% NaOH/60% ethanol at room temperature. Next, seedlings were rehydrated by successive incubations in 40%, 20% and 10% ethanol for 5 min, followed by incubation in a chloral hydrate (Fluka) buffer. Finally, seedlings were mounted in chloral hydrate and imaged by differential interference contrast microscopy with a BX51 microscope (Olympus, with a DP26 Olympus camera). Images were processed in ImageJ.

Confocal imaging

Confocal laser-scanning micrographs were obtained with a Zeiss LSM700 with a 488-nm argon laser line for excitation of GFP fluorescence. Emissions were detected between 505 and 580 nm. Using a 20× air objective, confocal scans were performed with the pinhole at 1 Airy unit. Localization was examined by confocal *z*-sectioning. Each image represents either a single focal plane or a projection of individual images taken as a *z*-series. *z*-stacking was performed by collecting images through the cortex and epidermal layers. Full *z*-stack confocal images were 3D-projected using ImageJ software. At least ten seedlings were analyzed per treatment. Images were processed in ImageJ.

Expression analysis by RT-qPCR

Embryos from stratified seeds or green siliques were peeled in a sterile hood using a stereomicroscope and incubated in MS plates with the indicated treatment in the dark. Around 150 embryos per sample were harvested after 24 days or 48 h of growth and frozen in liquid nitrogen. Tissue was ground using a ball mill (model MM400; Retsch) with 4-mm diameter balls in a 2-ml Eppendorf tube. Total RNA was isolated from embryos using an RNAeasy Plant Mini kit (Qiagen). During the extraction process, samples were treated with DNase according to the manufacturer's protocol (Qiagen). cDNA was prepared from 1 µg of total RNA with the iScript cDNA Synthesis Kit (Bio-Rad), dilutions of 1/10 were prepared and 1 µl was used in a 5-µl PCR reaction on a LightCycler 480 (Roche Diagnostics) with the SYBR Green I Master kit (Roche Diagnostics) according to the manufacturer's instructions. As control, non-RT-treated samples were included to test the purity of the cDNA. All experiments were performed with three technical replicates and three biological samples. The *PP2A* gene (At1g69960) was used as a control for normalization. Primer sequences can be found in Table S2.

Western blot analysis

Embryos from stratified seeds or green siliques were peeled in a sterile hood using a stereomicroscope and incubated in MS plates in the dark for 48 h. Then, around 250 embryos per sample were harvested and frozen in liquid nitrogen. Frozen tissue was ground with stainless steel 4-mm diameter balls in a 2-ml Eppendorf tube using a ball mill (model MM400; Retsch). Extraction buffer [100 mM Tris-HCl (pH 7.5), 25% (w/w, 0.81 M) sucrose, 5% (v/v) glycerol, 10 mM ethylenediaminetetraacetic acid (EDTA, pH 8.0), 10 mM ethyleneglycoltetraacetic acid (EGTA pH 8.0), 5 mM KCl and 1 mM 1,4-dithiothreitol (DTT)] was added to the frozen tissue. After Bradford quantification, 20 µg of protein were diluted in 20 µl of buffer and prepared for electrophoresis by adding 5 µl of loading buffer (5× SDS) and incubating at 45°C for 5 min. The electrophoresis was performed in a commercial 10% Mini-PROTEAN TGX Precast Protein Gels (Bio-Rad) at 35 mA. Transference was carried out by a semidry system with a Trans-blot turbo transfer pack PVDF (Bio-Rad). The blot was washed in TBST buffer (Tris buffered saline and 0.05% Tween 20) + 5% milk powder, and blocked overnight in the same buffer at 4°C. Hybridization was carried out using an anti-GFP antibody (mouse monoclonal, Sigma-Aldrich, G6539, 1:7000) in TBST for 2 h at room temperature. The blot was washed three times for 10 min each wash with TBST+5% milk powder and afterwards hybridized with peroxidase-linked anti-mouse antibody (anti-mouse-HRP from GE Healthcare, NA9310, 1:15,000) in TBST for 1 h. Finally, three washes in TBST and one in water were performed, prior to visualization using the SuperSignal West Femto Maximum Sensitivity Substrate kit (Thermo Scientific) and analysis using an Amersham Imager 600 (GE Healthcare).

Accession numbers

Sequence data from this article can be found in the Arabidopsis Genome Initiative or GenBank/EMBL databases under the following accession numbers: At1g73590 (PIN1), At5g57090 (PIN2), At1g70940 (PIN3), At2g01420 (PIN4), At1g23080 (PIN7), At1g52340 (ABA2), At4g37580 (HLS1), At4g23100 (RML1), At3g53420 (PIP2).

Acknowledgements

We thank Jiri Friml and Phillip Brewer for inspiring discussion and for help in preparing the manuscript. This research was supported by the Scientific Service Units (SSU) of IST-Austria through resources provided by the Bioimaging Facility (BIF), the Life Science Facility (LSF).

Competing interests

The authors declare no competing or financial interests.

Author contributions

Conceptualization: Q.Z., M.G., E.B.; Methodology: Q.Z., M.G., J.P., P.Z., M.S.; Validation: Q.Z., M.G., E.B.; Formal analysis: Q.Z., M.G., E.B.; Investigation: Q.Z., M.G., J.P., P.Z.; Resources: J.P., P.Z., M.S., E.B.; Writing - original draft: Q.Z., M.G., E.B.; Writing - review & editing: Q.Z., M.G., E.B.; Visualization: Q.Z., M.G., E.B.; Supervision: E.B.; Project administration: E.B.; Funding acquisition: M.S., E.B.

Funding

This work was supported by grants from the European Research Council (Starting Independent Research Grant ERC-2007-Stg- 207362-HCPO to E.B.). J.P. and M.S. received funds from European Regional Development Fund-Project 'Centre for Experimental Plant Biology' (No. CZ.02.1.01/0.0/0.0/16_019/0000738).

Supplementary information

Supplementary information available online at
http://dev.biologists.org/lookup/doi/10.1242/dev.175919.supplemental

References

Abbas, M., Alabadí, D. and Blázquez, M. A. (2013). Differential growth at the apical hook: all roads lead to auxin. *Front. Plant Sci.* **5**, 441. doi:10.3389/fpls.2013.00441

Benková, E., Michniewicz, M., Sauer, M., Teichmann, T., Seifertová, D., Jürgens, G. and Friml, J. (2003). Local, efflux-dependent auxin gradients as a common module for plant organ formation. *Cell* **115**, 591-602. doi:10.1016/S0092-8674(03)00924-3

Bennett, M. J., Marchant, A., Green, H. G., May, S. T., Ward, S. P., Millner, P. A., Walker, A. R., Schulz, B. and Feldmann, K. A. (1996). Arabidopsis AUX1 gene: a permease-like regulator of root gravitropism. *Science* **273**, 948-950. doi:10.1126/science.273.5277.948

Blilou, I., Xu, J., Wildwater, M., Willemsen, V., Paponov, I., Friml, J., Heidstra, R., Aida, M., Palme, K. and Scheres, B. (2005). The PIN auxin efflux facilitator network controls growth and patterning in Arabidopsis roots. *Nature* **433**, 39-44. doi:10.1038/nature03184

Brunoud, G., Wells, D. M., Oliva, M., Larrieu, A., Mirabet, V., Burrow, A. H., Beeckman, T., Kepinski, S., Traas, J., Bennett, M. J. et al. (2012). A novel sensor to map auxin response and distribution at high spatio-temporal resolution. *Nature* **482**, 103-106. doi:10.1038/nature10791

Cheng, J. C., Seeley, K. A. and Sung, Z. R. (1995). RML1 and RML2, Arabidopsis genes required for cell proliferation at the root tip. *Plant Physiol.* **107**, 365-376. doi:10.1104/pp.107.2.365

Cho, M. and Cho, H. T. (2012). The function of ABCB transporters in auxin transport. *Plant Signal. Behav.* **8**, e22990. doi:10.4161/psb.22990

Cutler, S. R., Ehrhardt, D. W., Griffitts, J. S. and Somerville, C. R. (2000). Random GFP::cDNA fusions enable visualization of subcellular structures in cells of Arabidopsis at a high frequency. *Proc. Natl Acad. Sci. USA* **97**, 3718-3723. doi:10.1073/pnas.97.7.3718

Darwin, C. and Darwin, F. (1881). *The Power of Movement in Plants*. Appleton and Co.: Kessinger Pub.

Delmas, F., Sankaranarayanan, S., Deb, S., Widdup, E., Bournonville, C., Bollier, N., Northey, J. G. B., McCourt, P. and Samuel, M. A. (2013). ABI3 controls embryo degreening through Mendel's I locus. *Proc. Natl. Acad. Sci. USA* **110**, E3888-E3894. doi:10.1073/pnas.1308114110

Dhonukshe, P., Aniento, F., Hwang, I., Robinson, D. G., Mravec, J., Stierhof, Y.-D. and Friml, J. (2007). Clathrin-mediated constitutive endocytosis of PIN auxin efflux carriers in Arabidopsis. *Curr. Biol.* **17**, 520-527. doi:10.1016/j.cub.2007.01.052

Finch-Savage, W. E. and Leubner-Metzger, G. (2006). Seed dormancy and the control of germination. *New Phytol.* **171**, 501-523. doi:10.1111/j.1469-8137.2006.01787.x

Forner, J. and Binder, S. (2007). The red fluorescent protein eqFP611: application in subcellular localization studies in higher plants. *BMC Plant Biol.* **7**, 28. doi:10.1186/1471-2229-7-28

Frey, A., Godin, B., Bonnet, M., Sotta, B. and Marion-Poll, A. (2004). Maternal synthesis of abscisic acid controls seed development and yield in Nicotiana plumbaginifolia. *Planta* **218**, 958-964. doi:10.1007/s00425-003-1180-7

Friml, J. (2003). Auxin transport - shaping the plant. *Curr. Opin. Plant Biol.* **6**, 7-12. doi:10.1016/S1369526602000031

Friml, J., Wiśniewska, J., Benková, E., Mendgen, K. and Palme, K. (2002). Lateral relocation of auxin efflux regulator PIN3 mediates tropism in Arabidopsis. *Nature* **415**, 806-809. doi:10.1038/415806a

Fukaki, H., Wysocka-Diller, J., Kato, T., Fujisawa, H., Benfey, P. N. and Tasaka, M. (1998). Genetic evidence that the endodermis is essential for shoot gravitropism in Arabidopsis thaliana. *Plant J.* **14**, 425-430. doi:10.1046/j.1365-313X.1998.00137.x

Gallego-Bartolomé, J., Arana, M. V., Vandenbussche, F., Žádníková, P., Minguet, E. G., Guardiola, V., Van Der Straeten, D., Benkova, E., Alabadí, D. and Blázquez, M. A. (2011). Hierarchy of hormone action controlling apical hook development in Arabidopsis. *Plant J.* **67**, 622-634. doi:10.1111/j.1365-313X.2011.04621.x

Galweiler, L., Guan, C., Muller, A., Wisman, E., Mendgen, K., Yephremov, A. and Palme, K. (1998). Regulation of polar auxin transport by AtPIN1 in Arabidopsis vascular tissue. *Science* **282**, 2226-2230. doi:10.1126/science.282.5397.2226

Ge, L. and Chen, R. (2016). Negative gravitropism in plant roots. *Nat. Plants* **2**, 16155. doi:10.1038/nplants.2016.155

Han, S.-Y., Kitahata, N., Sekimata, K., Saito, T., Kobayashi, M., Nakashima, K., Yamaguchi-Shinozaki, K., Shinozaki, K., Yoshida, S. and Asami, T. (2004). A novel inhibitor of 9-cis-epoxycarotenoid dioxygenase in abscisic acid biosynthesis in higher plants. *Plant Physiol.* **135**, 1574-1582. doi:10.1104/pp.104.039511

Harrison, B. R. and Masson, P. H. (2008). ARL2, ARG1 and PIN3 define a gravity signal transduction pathway in root statocytes. *Plant J.* **53**, 380-392. doi:10.1111/j.1365-313X.2007.03351.x

Jefferson, R. A., Kavanagh, T. A. and Bevan, M. W. (1987). GUS fusions: beta-glucuronidase as a sensitive and versatile gene fusion marker in higher plants. *EMBO J.* **6**, 3901-3907. doi:10.1002/j.1460-2075.1987.tb02730.x

Kleine-Vehn, J., Leitner, J., Zwiewka, M., Sauer, M., Abas, L., Luschnig, C. and Friml, J. (2008). Differential degradation of PIN2 auxin efflux carrier by retromer-dependent vacuolar targeting. *Proc. Natl. Acad. Sci. USA* **105**, 17812-17817. doi:10.1073/pnas.0808073105

Kleine-Vehn, J., Ding, Z., Jones, A. R., Tasaka, M., Morita, M. T. and Friml, J. (2010). Gravity-induced PIN transcytosis for polarization of auxin fluxes in gravity-sensing root cells. *Proc. Natl. Acad. Sci. USA* **107**, 22344-22349. doi:10.1073/pnas.1013145107

Kuhn, H. and Galston, A. W. (1992). Physiological asymmetry in etiolated pea epicotyls: relation to patterns of auxin distribution and phototropic behavior. *Photochem. Photobiol.* **55**, 313-318. doi:10.1111/j.1751-1097.1992.tb04243.x

Liu, X. and Hou, X. (2018). Antagonistic regulation of ABA and GA in metabolism and signaling pathways. *Front. Plant Sci.* **9**, 251. doi:10.3389/fpls.2018.00251

Luschnig, C., Gaxiola, R. A., Grisafi, P. and Fink, G. R. (1998). EIR1, a root-specific protein involved in auxin transport, is required for gravitropism in Arabidopsis thaliana. *Genes Dev.* **12**, 2175-2187. doi:10.1101/gad.12.14.2175

MacDonald, I. R., Gordon, D. C., Hart, J. W. and Maher, E. P. (1983). The positive hook: the role of gravity in the formation and opening of the apical hook. *Planta* **158**, 76-81. doi:10.1007/BF00395406

Marhavý, P., Bielach, A., Abas, L., Abuzeineh, A., Duclercq, J., Tanaka, H., Pařezová, M., Petrášek, J., Friml, J., Kleine-Vehn, J. et al. (2011). Cytokinin modulates endocytic trafficking of PIN1 auxin efflux carrier to control plant organogenesis. *Dev. Cell* **21**, 796-804. doi:10.1016/j.devcel.2011.08.014

Mazzella, M. A., Casal, J. J., Muschietti, J. P. and Fox, A. R. (2014). Hormonal networks involved in apical hook development in darkness and their response to light. *Front. Plant Sci.* **5**, 52. doi:10.3389/fpls.2014.00052

Miyamoto, K., Yamasaki, T., Uheda, E. and Ueda, J. (2014). Analysis of apical hook formation in Alaska pea with a 3-D clinostat and agravitropic mutant ageotropum. *Front. Plant Sci.* **5**, 137. doi:10.3389/fpls.2014.00137

Müller, A., Guan, C., Gälweiler, L., Tänzler, P., Huijser, P., Marchant, A., Parry, G., Bennett, M., Wisman, E. and Palme, K. (1998). AtPIN2 defines a locus of Arabidopsis for root gravitropism control. *EMBO J.* **17**, 6903-6911. doi:10.1093/emboj/17.23.6903

Nakayama, N., Smith, R. S., Mandel, T., Robinson, S., Kimura, S., Boudaoud, A. and Kuhlemeier, C. (2012). Mechanical regulation of auxin-mediated growth. *Curr. Biol.* **22**, 1468-1476. doi:10.1016/j.cub.2012.06.050

Nambara, E., Nambara, E., McCourt, P. and Naito, S. (1995). A regulatory role for the ABI3 gene in the establishment of embryo maturation in Arabidopsis thaliana. *Development* **121**, 629-636.

Nambara, E., Kawaide, H., Kamiya, Y. and Naito, S. (1998). Characterization of an Arabidopsis thaliana mutant that has a defect in ABA accumulation: ABA-dependent and ABA-independent accumulation of free amino acids during dehydration. *Plant Cell Physiol.* **39**, 853-858. doi:10.1093/oxfordjournals.pcp.a029444

Ottenschlager, I., Wolff, P., Wolverton, C., Bhalerao, R. P., Sandberg, G., Ishikawa, H., Evans, M. and Palme, K. (2003). Gravity-regulated differential auxin transport from columella to lateral root cap cells. *Proc. Natl. Acad. Sci. USA* **100**, 2987-2991. doi:10.1073/pnas.0437936100

Ouellet, F., Overvoorde, P. J. and Theologis, A. (2001). IAA17/AXR3: biochemical insight into an auxin mutant phenotype. *Plant Cell* **13**, 829-841. doi:10.1105/tpc.13.4.829

Paciorek, T., Zažímalová, E., Ruthardt, N., Petrášek, J., Stierhof, Y.-D., Kleine-Vehn, J., Morris, D. A., Emans, N., Jürgens, G., Geldner, N. et al. (2005). Auxin inhibits endocytosis and promotes its own efflux from cells. *Nature* **435**, 1251-1256. doi:10.1038/nature03633

Peaucelle, A., Braybrook, S. A., Le Guillou, L., Bron, E., Kuhlemeier, C. and Höfte, H. (2011). Pectin-induced changes in cell wall mechanics underlie organ initiation in Arabidopsis. *Curr. Biol.* **21**, 1720-1726. doi:10.1016/j.cub.2011.08.057

Petrasek, J. and Friml, J. (2009). Auxin transport routes in plant development. *Development* **136**, 2675-2688. doi:10.1242/dev.030353

Raz, V. and Ecker, J. R. (1999). Regulation of differential growth in the apical hook of Arabidopsis. *Development* **126**, 3661-3668.

Raz, V. and Koornneef, M. (2001). Cell division activity during apical hook development. *Plant Physiol.* **125**, 219-226. doi:10.1104/pp.125.1.219

Rowe, J. H., Topping, J. F., Liu, J. and Lindsey, K. (2016). Abscisic acid regulates root growth under osmotic stress conditions via an interacting hormonal network with cytokinin, ethylene and auxin. *New Phytol.* **211**, 225-239. doi:10.1111/nph.13882

Sabatini, S., Beis, D., Wolkenfelt, H., Murfett, J., Guilfoyle, T., Malamy, J., Benfey, P., Leyser, O., Bechtold, N., Weisbeek, P. et al. (1999). An auxin-dependent distal organizer of pattern and polarity in the Arabidopsis root. *Cell* **99**, 463-472. doi:10.1016/S0092-8674(00)81535-4

Shkolnik-Inbar, D. and Bar-Zvi, D. (2010). ABI4 mediates abscisic acid and cytokinin inhibition of lateral root formation by reducing polar auxin transport in arabidopsis. *Plant Cell* **22**, 3560-3573. doi:10.1105/tpc.110.074641

Stamm, P., Topham, A. T., Mukhtar, N. K., Jackson, M. D. B., Tomé, D. F. A., Beynon, J. L. and Bassel, G. W. (2017). The transcription factor ATHB5 affects

GA-mediated plasticity in hypocotyl cell growth during seed germination. *Plant Physiol.* **173**, 907-917. doi:10.1104/pp.16.01099

Stepanova, A. N., Robertson-Hoyt, J., Yun, J., Benavente, L. M., Xie, D.-Y., Doležal, K., Schlereth, A., Jürgens, G. and Alonso, J. M. (2008). TAA1-mediated auxin biosynthesis is essential for hormone crosstalk and plant development. *Cell* **133**, 177-191. doi:10.1016/j.cell.2008.01.047

Swarup, R. and Péret, B. (2012). AUX/LAX family of auxin influx carriers-an overview. *Front. Plant Sci.* **3**, 225. doi:10.3389/fpls.2012.00225

Swarup, R., Kramer, E. M., Perry, P., Knox, K., Leyser, H. M. O., Haseloff, J., Beemster, G. T. S., Bhalerao, R. and Bennett, M. J. (2005). Root gravitropism requires lateral root cap and epidermal cells for transport and response to a mobile auxin signal. *Nat. Cell Biol.* **7**, 1057-1065. doi:10.1038/ncb1316

Ueda, J., Miyamoto, K., Yuda, T., Hoshino, T., Sato, K., Fujii, S., Kamigaichi, S., Izumi, R., Ishioka, N., Aizawa, S. et al. (2000). STS-95 space experiment for plant growth and development, and auxin polar transport. *Uchu Seibutsu Kagaku* **14**, 47-57. doi:10.2187/bss.14.47

Uyttewaal, M., Traas, J. and Hamant, O. (2010). Integrating physical stress, growth, and development. *Curr. Opin. Plant Biol.* **13**, 46-52. doi:10.1016/j.pbi.2009.10.004

Uyttewaal, M., Burian, A., Alim, K., Landrein, B., Borowska-Wykręt, D., Dedieu, A., Peaucelle, A., Ludynia, M., Traas, J., Boudaoud, A. et al. (2012). Mechanical stress acts via katanin to amplify differences in growth rate between adjacent cells in Arabidopsis. *Cell* **149**, 439-451. doi:10.1016/j.cell.2012.02.048

Vandenbussche, F., Petrasek, J., Zadnikova, P., Hoyerova, K., Pesek, B., Raz, V., Swarup, R., Bennett, M., Zazimalova, E., Benkova, E. et al. (2010). The auxin influx carriers AUX1 and LAX3 are involved in auxin-ethylene interactions during apical hook development in Arabidopsis thaliana seedlings. *Development* **137**, 597-606. doi:10.1242/dev.040790

Vieten, A., Vanneste, S., Wisniewska, J., Benkova, E., Benjamins, R., Beeckman, T., Luschnig, C. and Friml, J. (2005). Functional redundancy of PIN proteins is accompanied by auxin-dependent cross-regulation of PIN expression. *Development* **132**, 4521-4531. doi:10.1242/dev.02027

Xu, J. and Scheres, B. (2005). Dissection of arabidopsis ADP-RIBOSYLATION FACTOR 1 function in epidermal cell polarity. *Plant Cell* **17**, 525-536. doi:10.1105/tpc.104.028449

Yang, L., Zhang, J., He, J., Qin, Y., Hua, D., Duan, Y., Chen, Z. and Gong, Z. (2014). ABA-mediated ROS in mitochondria regulate root meristem activity by controlling PLETHORA expression in arabidopsis. *PLoS Genet.* **10**, e1004791. doi:10.1371/journal.pgen.1004791

Yoshihara, T. and Spalding, E. P. (2017). LAZY genes mediate the effects of gravity on auxin gradients and plant architecture. *Plant Physiol.* **175**, 959-969. doi:10.1104/pp.17.00942

Žádníková, P., Petrasek, J., Marhavy, P., Raz, V., Vandenbussche, F., Ding, Z., Schwarzerova, K., Morita, M. T., Tasaka, M., Hejatko, J. et al. (2010). Role of PIN-mediated auxin efflux in apical hook development of Arabidopsis thaliana. *Development* **137**, 607-617. doi:10.1242/dev.041277

Žádníková, P., Wabnik, K., Abuzeineh, A., Gallemi, M., Van Der Straeten, D., Smith, R. S., Inzé, D., Friml, J., Prusinkiewicz, P. and Benková, E. (2016). A model of differential growth-guided apical hook formation in plants. *Plant Cell* **28**, 2464-2477. doi:10.1105/tpc.15.00569

Zhu, Q., Žádníková, P., Smet, D., Van Der Straeten, D. and Benková, E. (2017). Real-time analysis of the apical hook development. *Methods Mol. Biol.* **1497**, 1-8. doi:10.1007/978-1-4939-6469-7_1

Supplementary Materials and methods for abamine synthesis

General information

All starting materials were used as received from commercial sources without further purification. All reactions were performed in round-bottom flasks fitted with rubber septa using the standard laboratory techniques. Reactions sensitive to air and/or moisture were performed under a positive pressure of argon. Analytical thin-layer chromatography (TLC) was performed using aluminum plates pre-coated with silica gel (silica gel 60 F254). TLC plates were visualized by exposure to ultraviolet light and then were stained by submersion in basic potassium permanganate solution or in ethanolic phosphomolybdic acid solution followed by brief heating. Column chromatography was performed on silica gel 60 (40-63 μm). Melting points (mp) were tested on a capillary melting point apparatus. ^{1}H NMR and ^{13}C NMR spectra were recorded on 500 and 125 MHz in $CDCl_3$; chemical shifts (δ ppm) and coupling constants (Hz) of ^{1}H NMR are reported in a standard fashion with relative to the remaining $CHCl_3$ present in $CDCl_3$ (δH = 7.27 ppm). ^{13}C NMR chemical shifts (δ ppm) are reported relative to $CHCl_3$ (δC = 77.23 ppm, central line of triplet). Proton coupling patterns are represented as singlet (s), doublet (d), doublet of doublet (dd), triplet (t), triplet of triplet (tt) and multiplet (m). HRMS data were obtained using quadrupole/ion trap mass analyzer. Analysis and assignments were made by comparison with literature spectroscopic data or using 2D-COSY, HSQC, HMBC, 2D-NOESY and 1D-NOEdiff experiments. The purity of **Aba** was determined by LC-MS (Acquity UPLC™ System, Waters, Milford, MA, USA) consisting of a binary solvent manager and sample manager). Reverse-phased column (Symetry C18, 5μm, 150 mm × 2.1 mm; Waters, Milford, MA, USA). The compound was separated in a linear gradient of MeOH (B) and 15mM ammonium formate adjusted to pH 4.0 (A) at a flow rate of 200 μl/min. Following binary gradient was used: 0 min, 10 % B; 0-24 min. linear gradient to 90 % B; 25-34 min. isocratic elution of 90 % B; 35-45 min. linear gradient to 10 % B. The column was kept at 25 °C. The effluent was introduced then to PDA detector (scanning range 210-700 nm with 1.2 nm resolution) and an electrospray source (source temperature 120 °C, desolvation temperature 300 °C, capillary voltage 3 kV, cone voltage 20 V). Nitrogen was used as well as cone gas (50 l/h) and desolvation gas (500 l/h). Data acquisition was performed in the full scan mode (50-1000 Da), scan time of 0.5 sec. and collision energy of 6 V. Analyses were performed in positive mode (ESI^{+}).

Synthesis overview

Targeted molecule was prepared using modified literature protocol in accessed in 7 steps and 17.5% overall yield (Han et al., 2004).

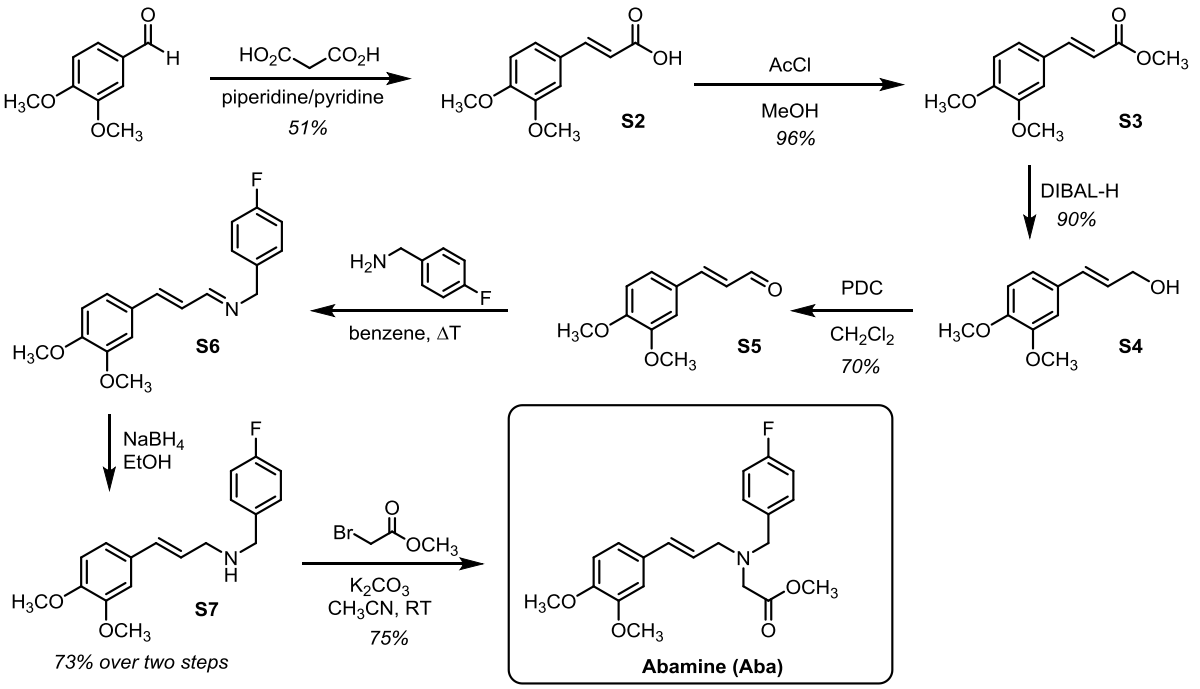

Experimental Protocols

Transformation of aldehyde to methyl ester **S3**

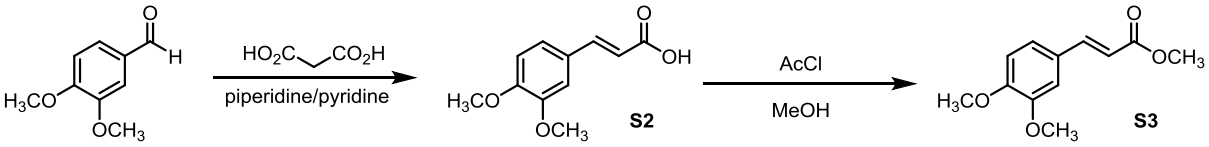

A solution of veratraldehyde (7.0 g, 42.1 mmol, 1.0 equiv) and malonic acid (5.2 g, 63.2 mmol, 1.5 equiv) in pyridine (12 mL, 3.5M to aldehyde) was stirred at RT for 5 min. Piperidine (629 μL, 6.4 mmol, 0.15 equiv) was added and the resulting mixture was stirred at 85°C in Schlenck tube for 8.5h. The resulting mixture was cooled to RT and the Schlenck tube was carefully opened and its contain was poured into ice/water bath (100g/150 mL placed in 500mL beaker). The resulting mixture was vigorously stirred and acid **S2** started to precipitate. When the ice melted, the resulting precipitate was filtered and dried under the vacuum at 30°C yielding acid **S2** (4.49g, 51%) in form of white crystals (m.p. = 178-180°C (from water)); ^{1}H NMR (500 MHz, $CDCl_3$) δ (ppm): 7.75 (d, J = 15.9 Hz, 1H), 7.15 (dd, J = 8.6, 2.0 Hz, 1H), 7.09 (d, J = 2.0 Hz, 1H), 6.89 (d, J = 8.4 Hz, 1H), 6.34 (d, J = 15.9 Hz, 1H), 3.93 (d, J = 0.6 Hz, 6H); ^{13}C NMR (126 MHz, $CDCl_3$) δ (ppm): 172.80, 151.71, 149.44, 147.21, 127.21, 123.37, 115.08, 111.20, 109.92, 56.20, 56.10.

Acid **S2** (4.49g, 21.56 mmol, 1.0 equiv) was dissolved in methanol (21mL, 1.0M) and the whole mixture was cooled to 0°C. Acetyl chloride (1.22 mL, 17.24 mmol, 0.8 equiv) was added and the whole mixture was allowed to warm to RT and stirred at RT for additional 12h. The whole mixture was evaporated under reduced pressure and the residue was purified by column chromatography on silica gel (P.E.:EtOAc = 2:1) yielding the desired ester **S3** as colorless solid (4.6g, 96%). M.p. = 64.5-65.5°C; ^{1}H NMR (500 MHz, $CDCl_3$) δ (ppm): 7.63 (d, J = 16.2 Hz, 1H), 7.10 (dd, J = 8.3, 1.8 Hz, 1H), 7.04 (d, J = 2.1 Hz, 1H), 6.86 (d, J = 8.6 Hz, 1H), 6.31 (d, J = 15.9 Hz, 1H), 3.90 (s, J = 4.6 Hz, 6H), 3.79 (s, 3H); ^{13}C NMR (126 MHz, $CDCl_3$) δ (ppm): 167.84, 151.26, 149.34, 144.96, 127.49, 122.77, 115.61, 111.15, 109.72, 56.12, 56.02, 51.79.

Ester S3 reduction to 3,4-dimethoxycinnamyl alcohol (S4)

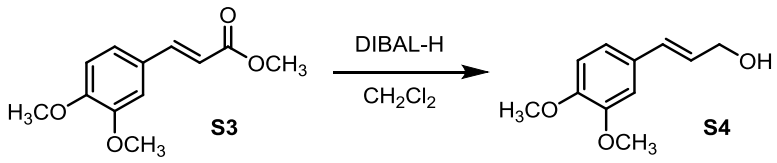

A solution of ester **S3** (3.3g, 13.49mmol, 1.0 equiv) in dry CH_2Cl_2 (27mL, 0.5M) was cooled to 0°C and DIBAL-H (33.7mL, 33.7mmol, 2.5 equiv; 1.0M solution in CH_2Cl_2) was added dropwise. The resulting mixture was stirred at 0°C for 30 min prior the cooling bath removal. After 1h at RT, the reaction mixture was again cooled to 0°C and stirred for 15 min at 0°C. Aqueous saturated solution of Rochel salt (10mL) was added dropwise to quench the reaction and the resulting mixture was stirred at RT for next 13h (milky suspension turned into the clear biphasic solution). Resulting phases were separated and the aqueous layer was extracted with CH_2Cl_2 (3x75mL). Combined organic layers were washed with brine (50mL), dried over Na_2SO_4, filtered and evaporated under reduced pressure. The residue was purified by column chromatography (silica gel; P.E.:EtOAc = 2:1) yielding the desired product **S4** (2.60g, 98%) as colorless solid. M.p. = 76-77°C; ^{1}H NMR (500 MHz, $CDCl_3$) δ (ppm): 6.97 – 6.91 (m, 2H), 6.83 (d, J = 8.3 Hz, 1H), 6.56 (d, J = 15.9 Hz, 1H), 6.26 (dt, J = 15.9, 6.1 Hz, 1H), 4.32 (dd, J = 6.1, 1.5 Hz, 2H), 3.91 (s, 3H), 3.89 (s, 3H); ^{13}C NMR (126 MHz, $CDCl_3$) δ (ppm): 149.20, 149.09, 131.37, 129.89, 126.71, 119.89, 111.25, 108.97, 64.06, 56.10, 56.00.

Transformation of 3,4-dimethoxycinnamyl alcohol S4 to aldehyde S5

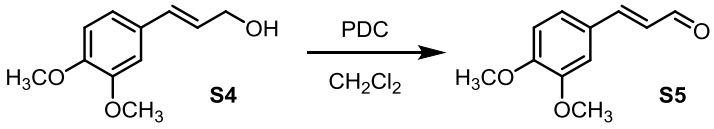

3,4-dimethoxycinnamyl alcohol (**S4**) (1.00 g, 5.1 mmol) in CH_2Cl_2 (10mL) was slowly added via syringe to a mixture of pyridinium dichromate (PDC, 3.86g, 10.3 mmol, 2.0 equiv) in CH_2Cl_2 (20mL). Resulting mixture was stirred for 2 h at RT prior 0.5 mL of methanol was added. The whole mixture was passed through silica gel (filtration) and filter cake was washed with EtOAc (300mL). Organic solvents were removed under reduced pressure and the crude aldehyde was purified by column chromatography (silica gel; P.E.:EtOAc = 4:1) yielding a desired aldehyde **S5** (690mg, 70%) as viscose oil. ^{1}H NMR (500 MHz, $CDCl_3$) δ (ppm): 9.66 (d, J = 7.9 Hz, 1H), 7.42 (d, J = 15.9 Hz, 1H), 7.17 (dd, J = 8.4, 2.0 Hz, 1H), 7.08 (d, J = 2.1 Hz, 1H), 6.91 (d, J = 8.3 Hz, 1H), 6.61 (dd, J = 15.9, 7.6 Hz, 1H), 3.94 (s, 3H), 3.93 (s, 3H); ^{13}C NMR (126 MHz, $CDCl_3$) δ (ppm) 193.78, 153.07, 152.14, 149.54, 127.22, 126.88, 123.64, 111.27, 109.97, 56.22, 56.11; MS (APCI, *m/z*, %): 193 (100) $[M+H]^+$, 210 (26) $[M+NH_4]^+$.

Transformation of 3,4-dimethoxycinnamyl aldehyde S5 to amine S7

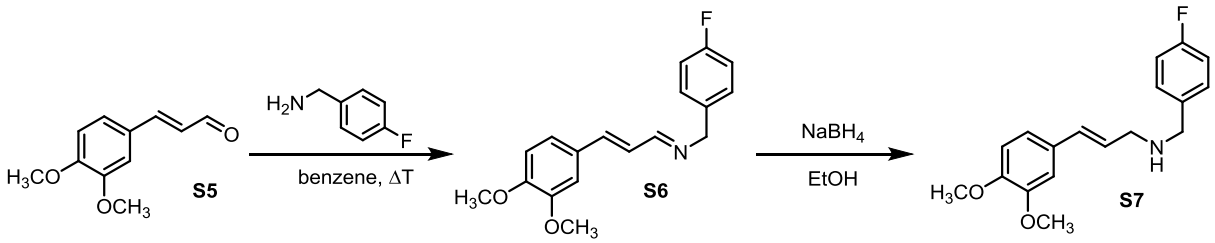

Aldehyde **S5** (690mg, 3.58mmol, 1.0 equiv) was dissolved in benzene (7.2mL, 0.5M) at RT and 4-fluorobenzylamine (429μL, 3.76 mmol, 1.05 equiv) was added. The resulting mixture was stirred at 80°C for 2h. The resulting mixture was evaporated to dryness under vacuum, and the residue, crude imine **S6** was used in the next step.

Imine **S6** (crude material from the previous step) was dissolved in EtOH (12 mL, 0.3M) and the resulting mixture was cooled to 0°C (ice/water). $NaBH_4$ (147mg, 3.89mmol, 1.05equiv) was added portion wise and the resulting mixture was allowed to stir at RT for 2h. The reaction mixture was diluted with water (25mL) and the whole mixture was extracted with CH_2Cl_2 (3x25 mL). Combined organic layers were washed with water (10 mL), brine (10 mL), dried over anhydrous Na_2SO_4, filtered and concentrated under reduced pressure. The crude material was purified by column chromatography (silica gel; CH_2Cl_2:MeOH = 95:5) to give amine **S7** (810mg, 73%) as viscose oil. ^{1}H NMR (500 MHz, $CDCl_3$) δ (ppm): 7.32 (ddd, J = 6.4, 4.9, 2.0 Hz, 2H), 7.05 – 6.98 (m, 2H), 6.95 (d, J = 2.1 Hz, 1H), 6.91 (dd, J = 8.4, 2.0 Hz, 1H), 6.82 (t, J = 7.3 Hz, 1H), 6.48 (d, J = 15.9 Hz, 1H), 6.19 (dt, J = 15.6, 6.6 Hz, 1H), 5.30 (s, 1H), 3.92 (dd, J = 6.1, 2.8 Hz, 2H), 3.90 (s, 3H), 3.88 (s, 3H), 3.44 (dd, J = 12.4, 4.7 Hz, 1H), 3.41 (dd, J = 11.6, 4.0 Hz, 1H); ^{13}C NMR (126 MHz, $CDCl_3$) δ (ppm): 149.20, 148.90, 135.83, 131.72, 130.27, 130.04, 129.98, 126.14, 119.63, 115.51, 115.35, 111.26, 108.77, 56.10, 55.98, 52.65, 51.31.

Alkylation of amine S7 to yield abamine Aba

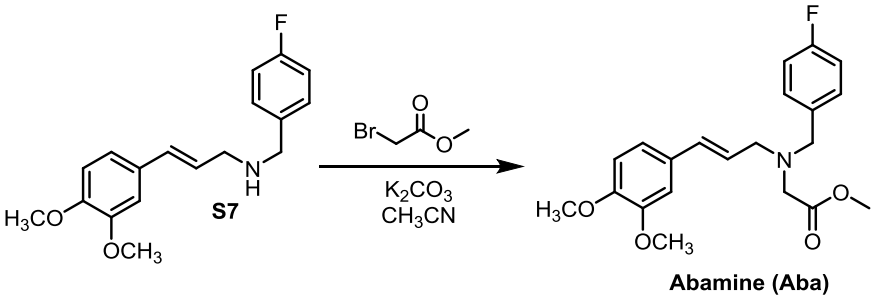

Benzylamine **S7** (810mg, 2.68 mmol, 1.0 equiv) was dissolved in CH_3CN (11 mL, 0.25M) and K_2CO_3 (742mg, 5.37 mmol, 2.0 equiv) was added. After 5 min, methyl bromoacetate (291µL, 3.08 mmol, 1.15 equiv) was added via syringe and the resulting mixture was stirred at RT for 14 h. The reaction mixture was then poured into sat. aq. $NaHCO_3$ (20 mL) and the whole mixture was extracted with CH_2Cl_2 (3x50mL). The combined organic phases were dried over Na_2SO_4, filtered and concentrated under reduced pressure. The resulting crude material was purified by column chromatography (SiO_2; P.E.:EtOAc = 4:1->2:1) yielding the desired abamine **Aba** (749mg, 75%) as colorless viscose oil.

^{1}H NMR (500 MHz, $CDCl_3$) δ (ppm) = 7.35 (dd, J = 8.6, 5.7 Hz, 2H), 7.02 (t, J = 8.7 Hz, 2H), 6.94 (d, J = 2.0 Hz, 1H), 6.90 (dd, J = 8.3, 2.0 Hz, 1H), 6.82 (d, J = 8.3 Hz, 1H), 6.48 (d, J = 15.9 Hz, 1H), 6.11 (dt, J = 15.9, 6.9 Hz, 1H), 3.90 (s, 3H), 3.89 (s, 3H), 3.78 (s, 2H), 3.68 (s, 3H), 3.39 (d, J = 6.1 Hz, 2H), 3.35 (s, 2H); ^{13}C NMR (126 MHz, $CDCl_3$) δ (ppm): 172.04, 149.22, 148.99, 133.07, 130.79, 130.73, 130.14, 125.16, 119.75, 115.41, 115.25, 111.24, 108.78, 57.66, 56.67, 56.13, 56.02, 53.93, 51.65; HRMS (ESI^+; *m/z*): $[M+H]^+$ = 374.74 amu. Elemental analysis: calculated for C21H24FNO4: C = 67.55%; H = 6.48%; N = 3.75; found: C = 67.85%; H = 6.65%; N = 3.48.

LC-MS (Acquity UPLC™ System, Waters, Milford, MA, USA) consisting of a binary solvent manager and sample manager). Reverse-phased column (Symetry C18, 5µm, 150 mm × 2.1 mm; Waters, Milford, MA, USA). The compound was separated in a linear gradient of MeOH (B) and 15mM ammonium formate adjusted to pH 4.0 (A) at a flow rate of 200 µl/min. Following binary gradient was used: 0 min, 10 % B; 0-24 min. linear gradient to 90 % B; 25-34 min. isocratic elution of 90 % B; 35-45 min. linear gradient to 10 % B. The column was kept at 25 °C. The effluent was introduced then to PDA detector (scanning range 210-700 nm with 1.2 nm resolution) and an electrospray source (source temperature 120 °C, desolvation temperature 300 °C, capillary voltage 3 kV, cone voltage 20 V). Nitrogen was used as well as cone gas (50 l/h) and desolvation gas (500 l/h). Data acquisition was performed in the full scan mode (50-1000 Da), scan time of 0.5 sec. and collision energy of 6 V.

Analyses were performed in positive mode (ESI+) therefore data were collected as quasi-molecular ions of [M+H]+. RT (abamine) = 27.90 min, $[M+H]^+$ = 374.74 amu. Purity 98.9%.

Abamine – Copy of ^{1}H and ^{13}C NMR spectra, LC chromatogram, and MS spectra

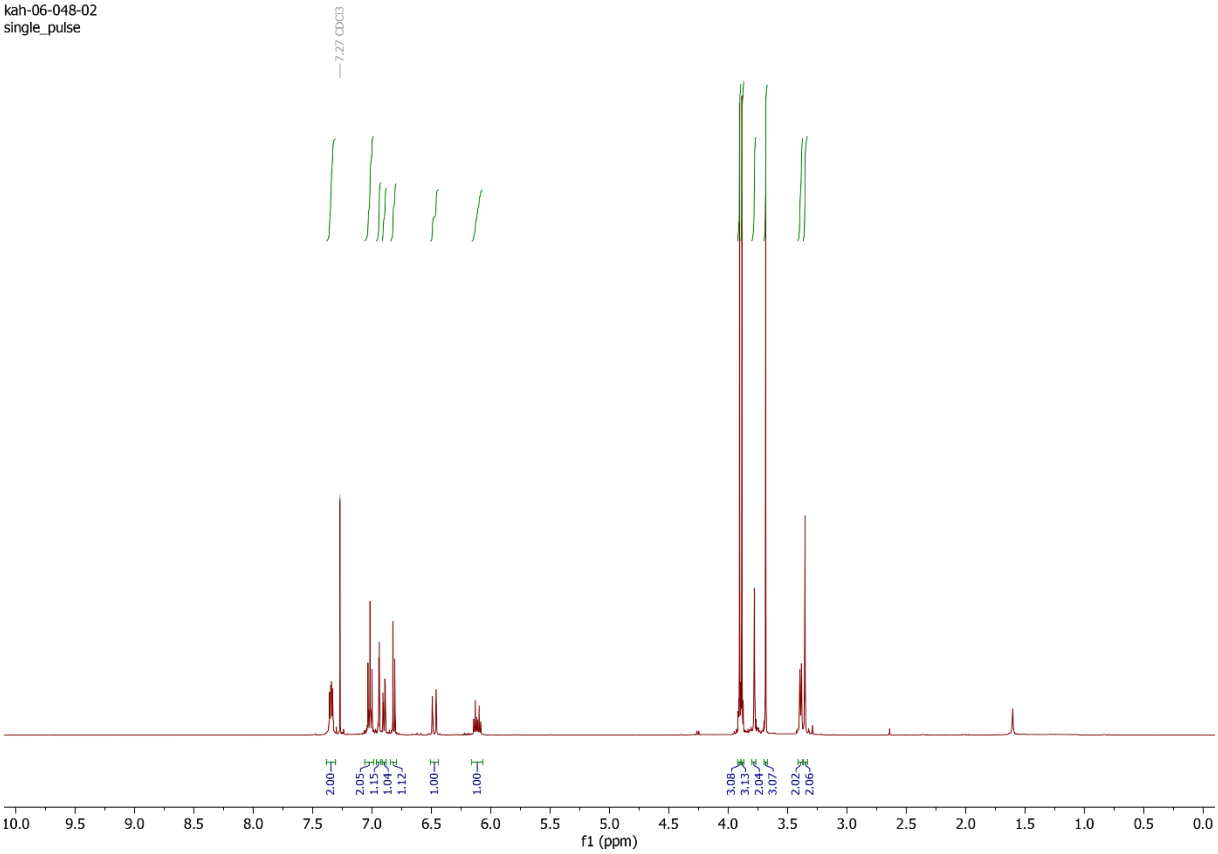

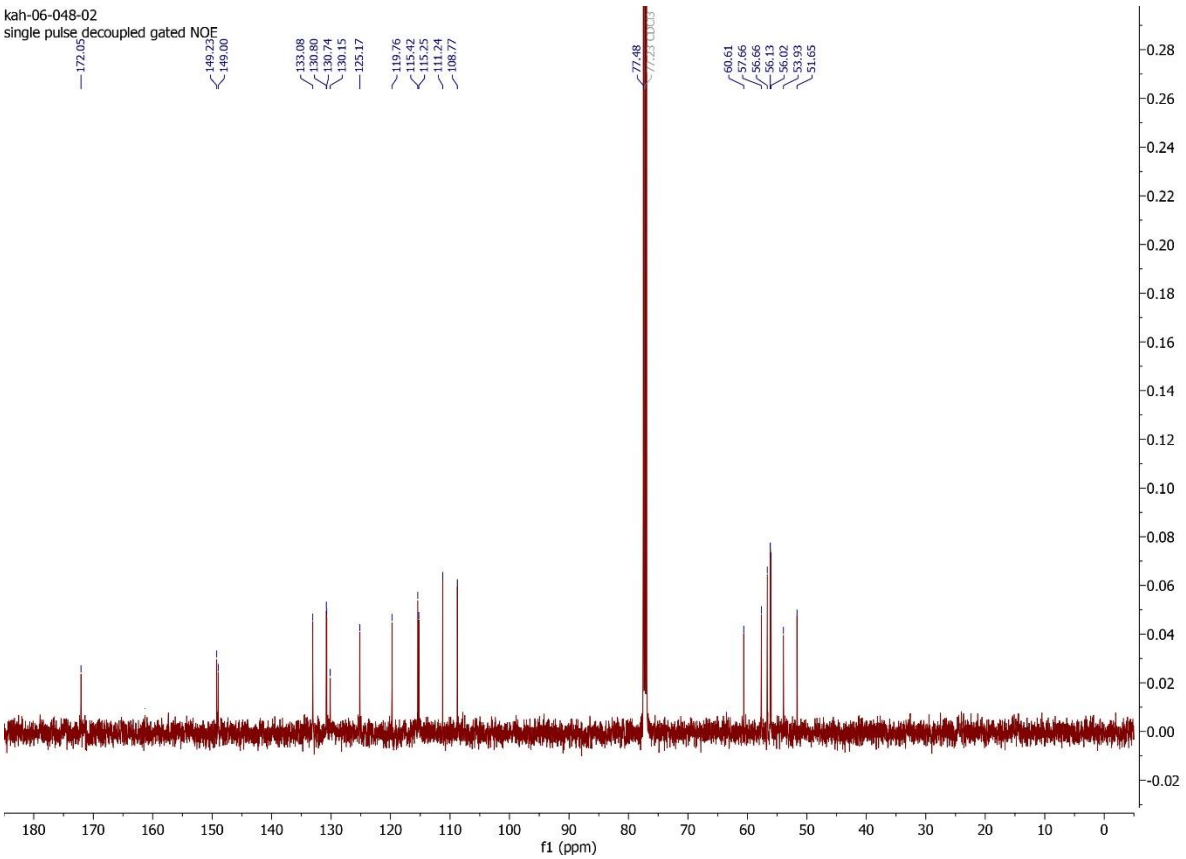

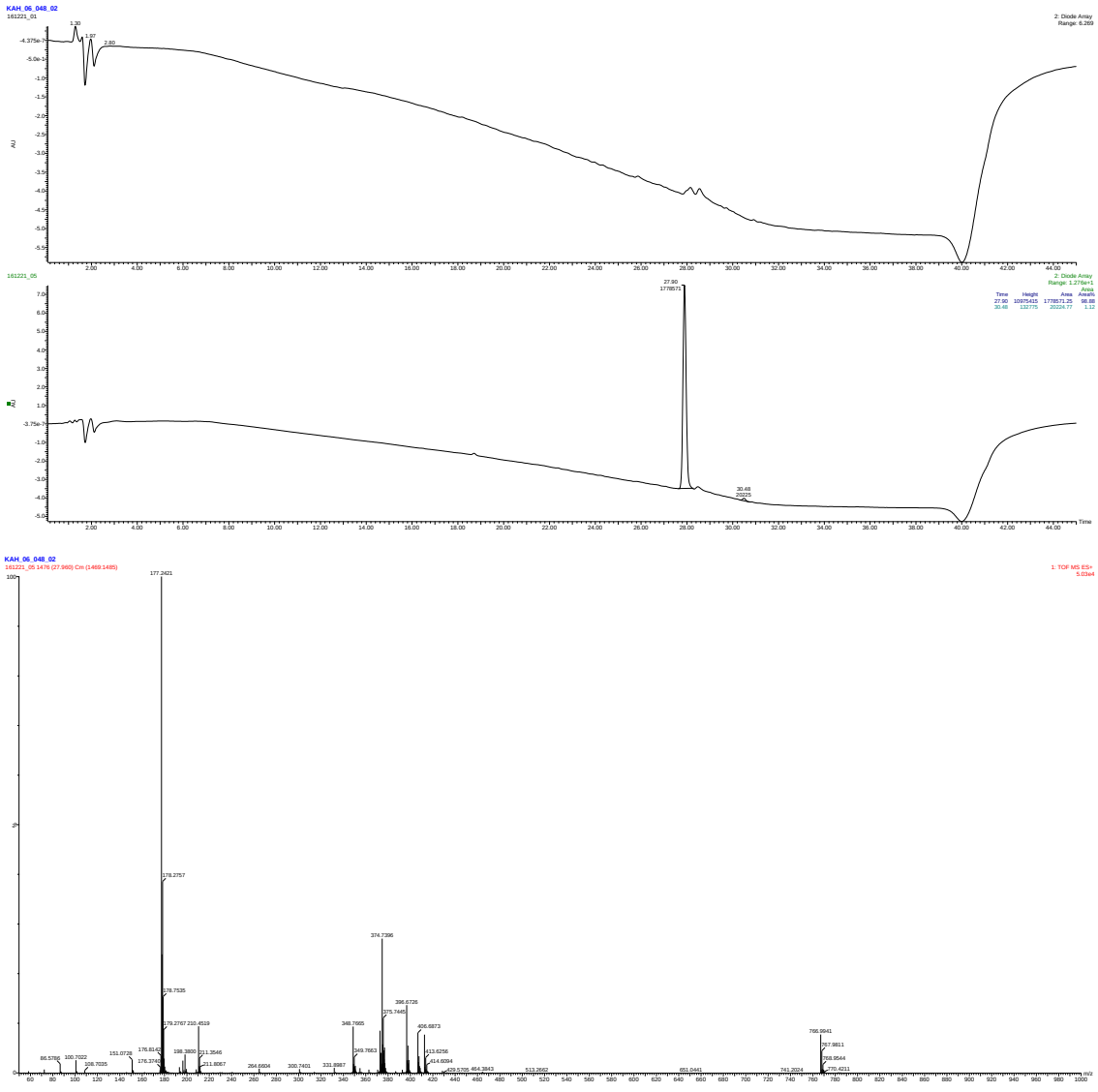

Han, S.-y., Kitahata, N., Saito, T., Kobayashi, M., Shinozaki, K., Yoshida, S., and Asami, T. (2004). A new lead compound for abscisic acid biosynthesis inhibitors targeting 9-cis-epoxycarotenoid dioxygenase. Bioorg. Med. Chem. Lett. **14,** 3033-3036.

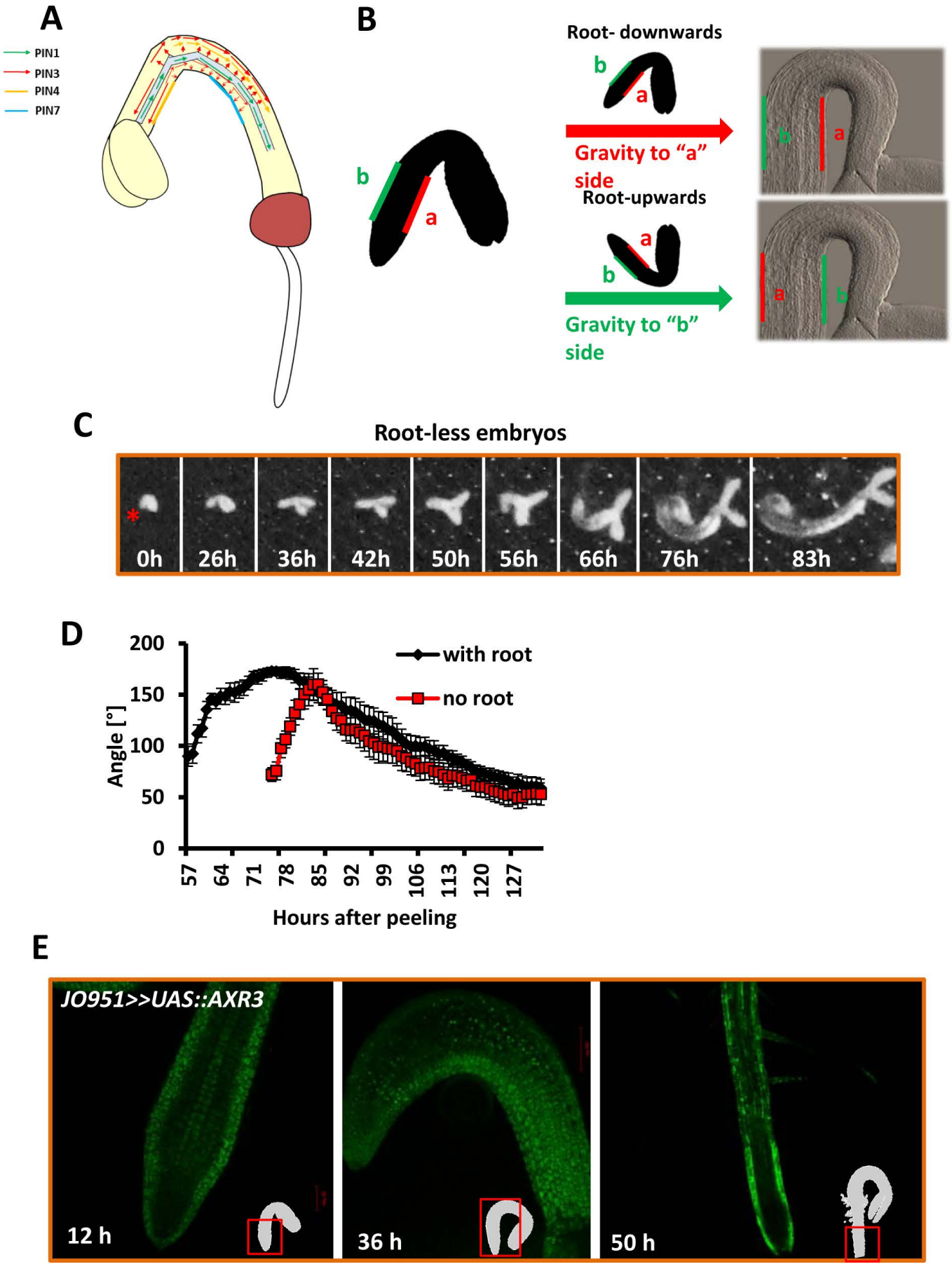

Figure S1. The root bending response to gravity guides the apical hook formation.

A. Model of auxin distribution during apical hook formation.

B. Scheme of mature embryos positioning to examine the impact of the embryonic shape on the apical hook formation. Mature embryos with the typical bent shape were dissected from seed coats and positioned on the media with root facing downwards or upwards. In the downwards and upwards orientation, either root side a or b, respectively, are gravity stimulated.

C-D. Real time monitoring of seedling growth after the embryonic root was detached. No apical hook formation could be detected (C). Kinetics of the apical hook development of intact and rootless seedlings (D). Red asterisk indicates the root pole position. Time in hours after transfer for incubation.

E. Expression analysis of J0951 activator using GFP reporter in roots of *J0951>>UAS::AXR3* seedlings. No GFP signal detected in roots at early phases of root growth (12 and 36h). 50h after start of incubation expression of GFP reporter at the root tip observed. Time in hours after transfer for incubation.

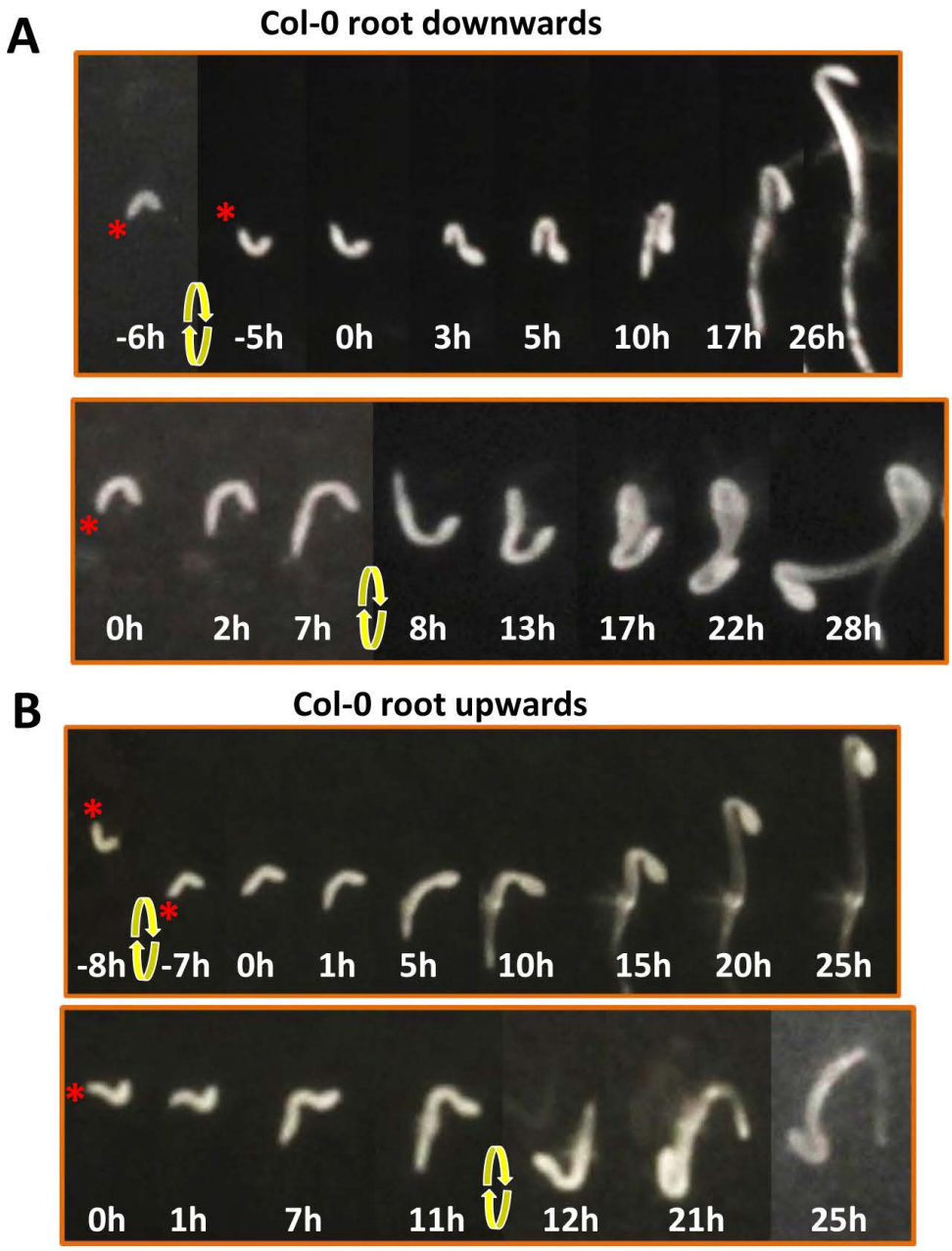

Figure S2. Root gravity driven bending coordinates the apical hook formation within a short developmental window.

A, B. Impact of changed gravity vector on the apical hook formation during germination of wild-type Col-0 seedlings. Seedlings positioned initially root down- (A) or upwards (B) were turned by 180 degrees at different time points. 0h indicates time of germination initiated by outgrowth of embryonic root and yellow arrows time of turning the plate. Red star indicates a root pole.

C,D. Real time monitoring of the apical hook formation in *scr-3* seedlings developing from mature embryos positioned in root downwards (A) and upwards (B) orientations. Time in hours after germination. Red star indicates a root pole.

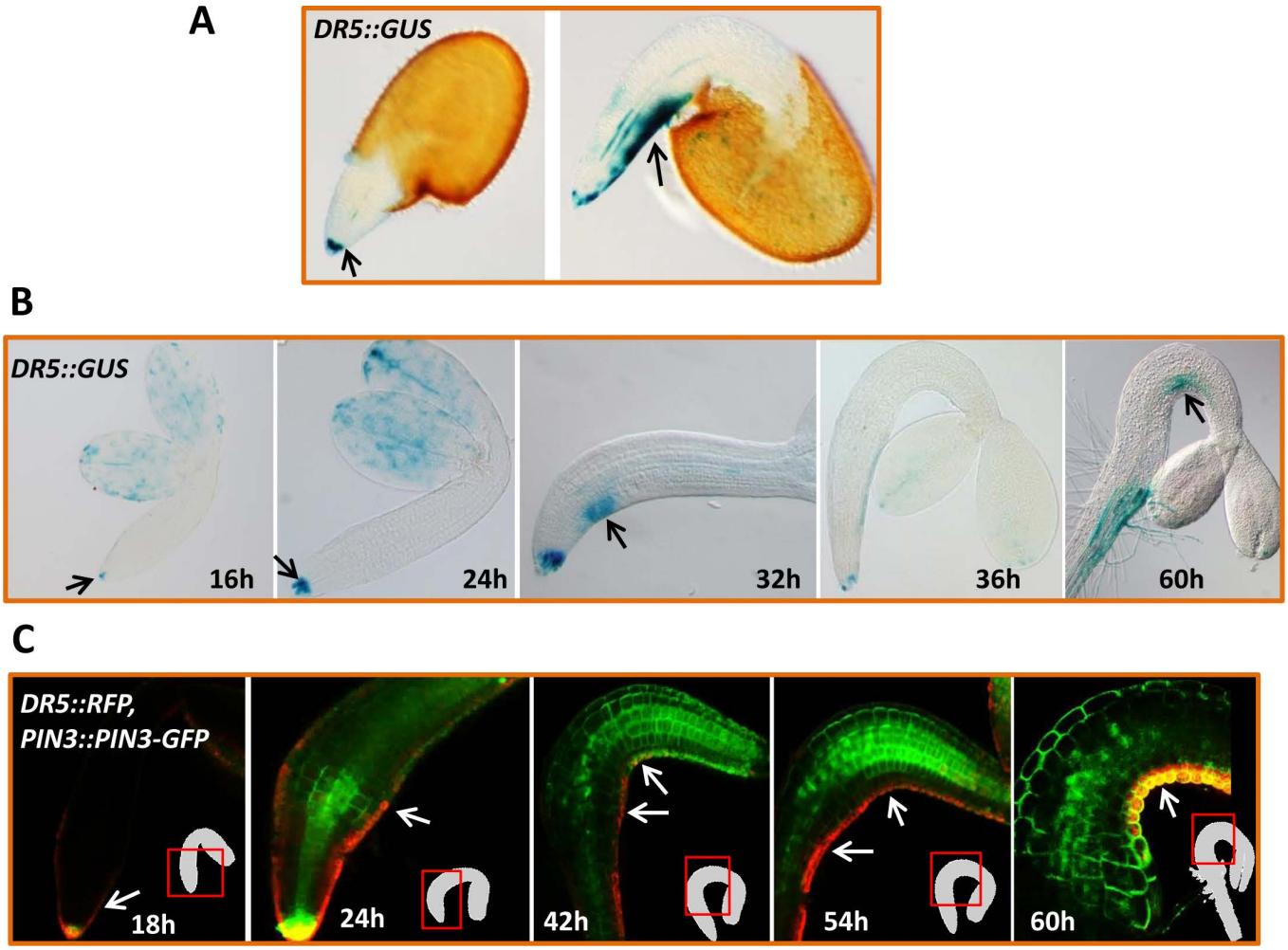

Figure S3. Monitoring of the auxin response during early phases of germination.

A. Auxin responses monitored using *DR5::GUS* reporter during early seed germination (radicle emergence). At first, auxin maximum detected in the root columella cells and afterwards at the gravi-stimulated side of the emerging root.

B. Monitoring of auxin responses during early phases of seedling development in darkness using *DR5::GUS* reporter. Auxin response maxima detected in the root columella (from 16h on). At 32h auxin response maximum observed at the root – hypocotyl junction, from 60h auxin response at the concave side of the apical hook detected.

C. Monitoring of the auxin response during early phases of seedlings developing in light using *DR5::RFP* reporter (red signal). Auxin maxima detected in the root columella (from 18h on). At 32h auxin response maximum detected at the root-hypocotyl junction, from 60h auxin response at the concave side of the apical hook detected. Green signal corresponds to *PIN3::PIN3-GFP* marker line. Time in hours after transfer for incubation (B,C.) Black (A, B) and white (C) arrows indicate the auxin response maximum.

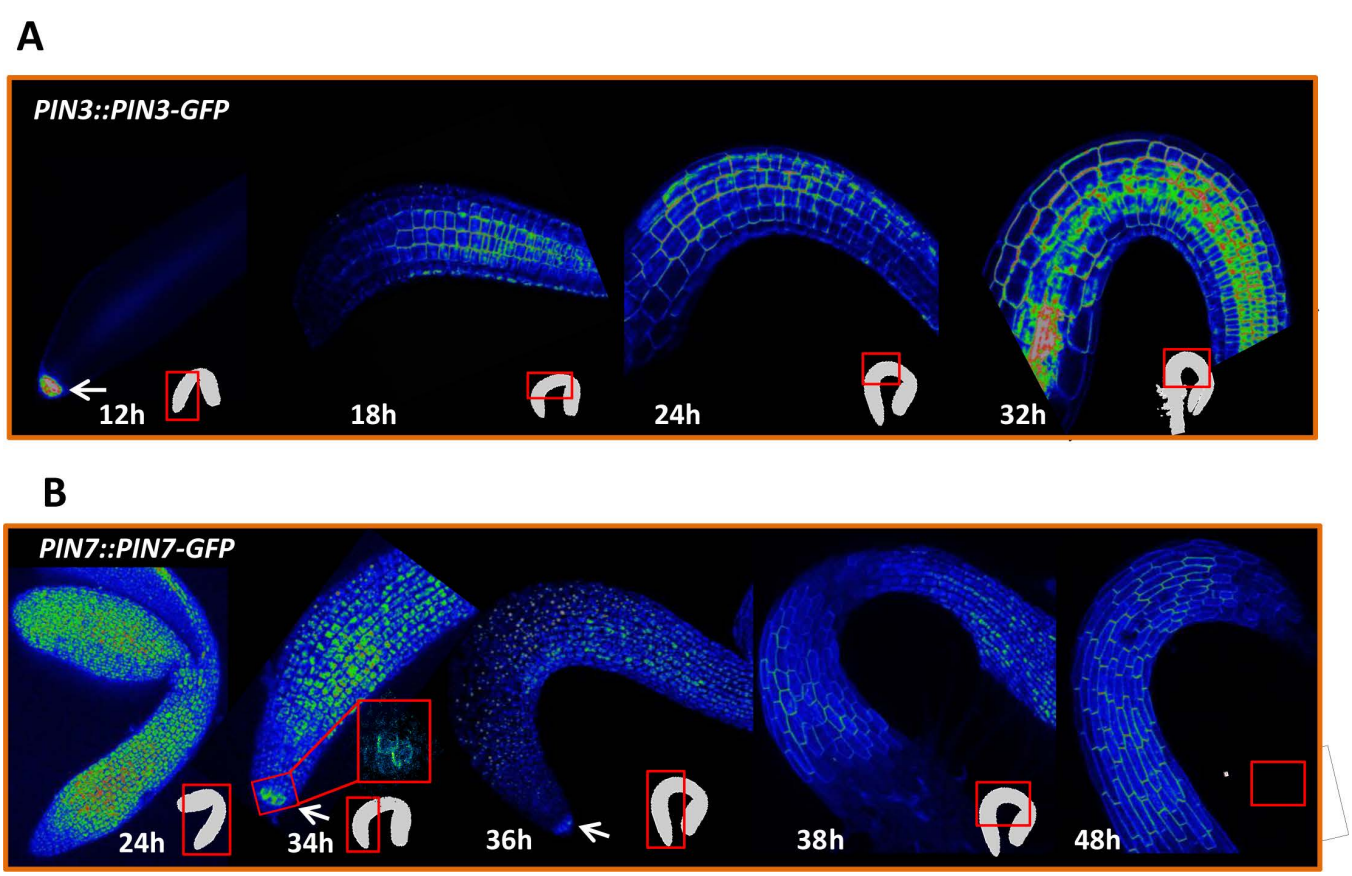

Figure S4. The expression pattern of PIN auxin efflux transporters during early phases of apical hook formation.

A. The earliest expression of *PIN3::PIN3-GFP* detected in the root columella cells at 12h after transfer for incubation. From 18h on PIN3-GFP detected in the hypocotyl, which progressively bends to form the apical hook.

B. Expression of *PIN7::PIN7-GFP* in the root columella detected 34h after transfer for incubation. PIN7-GFP in hypocotyl detected from 38h on.

White arrows indicate PIN-GFP signal in collumela. Insets indicate developmental stage of seedlings, red rectangle marks the zone magnified. Time in hours after transfer for incubation.

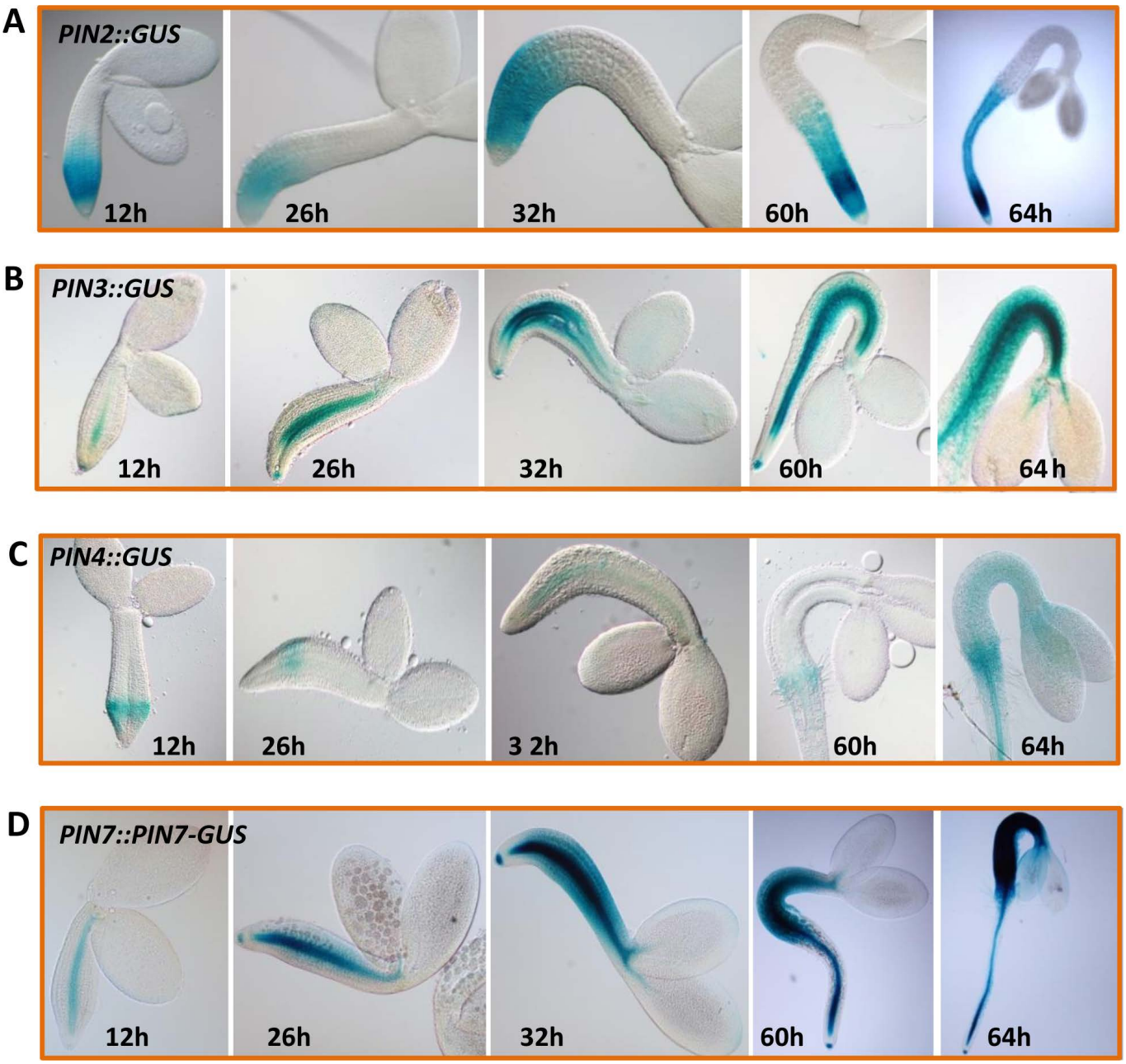

Figure S5. The pattern of *PINs* expression during early phases of the apical hook formation in darkness.

A-D. Monitoring of *PIN* genes (*PIN2::GUS* (A); *PIN3::GUS* (B); *PIN4::GUS* (C); and *PIN7::PIN7-GUS* (D)) expression during early phases of seedlings development. Time in hours after transfer for incubation.

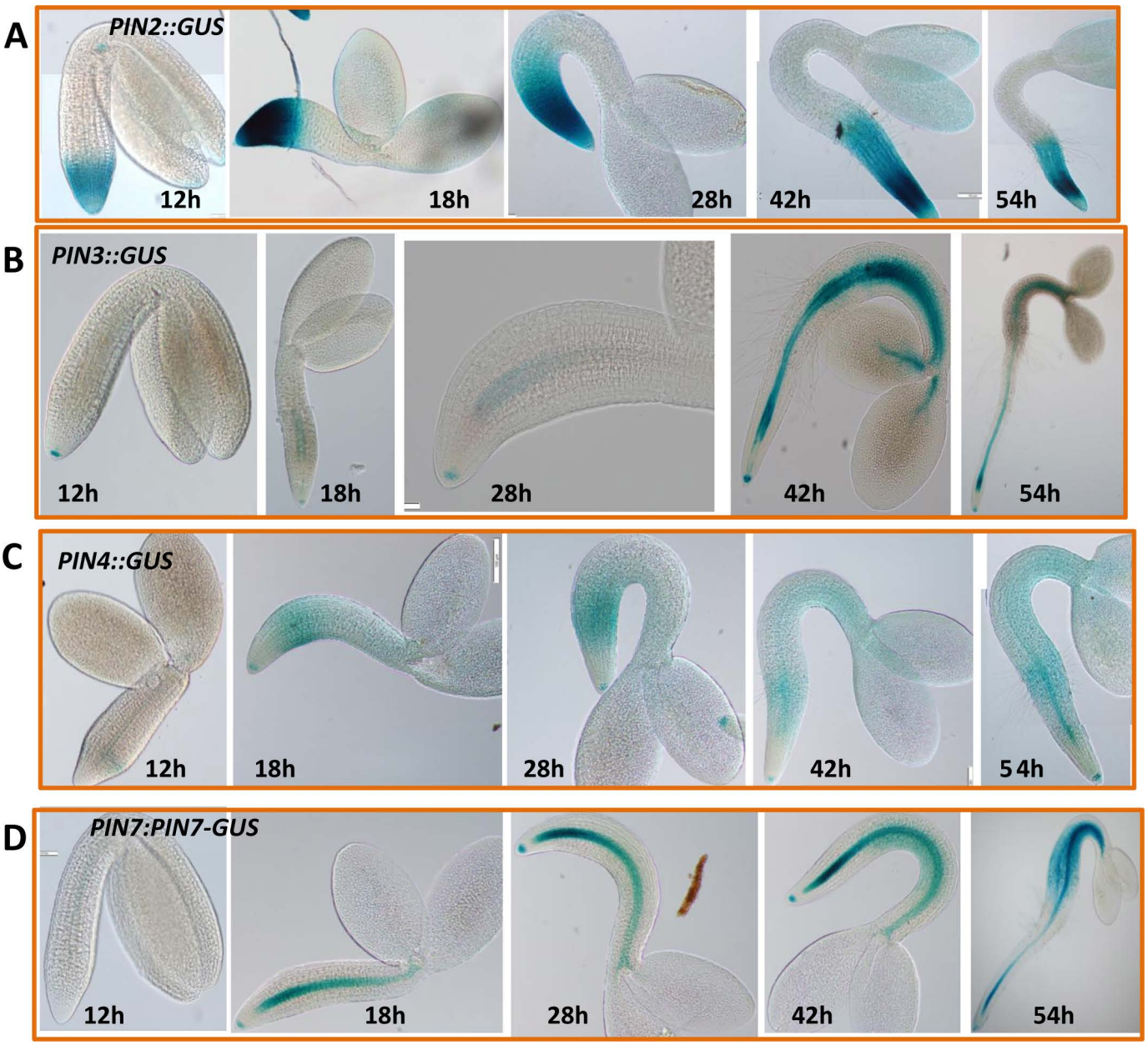

Figure S6. The pattern of *PINs* expression during early phases of the apical hook formation in light.

A-D. Monitoring of *PIN* genes (PIN2::GUS (A); *PIN3::GUS* (B); *PIN4::GUS* (C); and *PIN7::PIN7-GUS* (D)) expression during early phases of seedlings development. Time in hours after transfer for incubation.

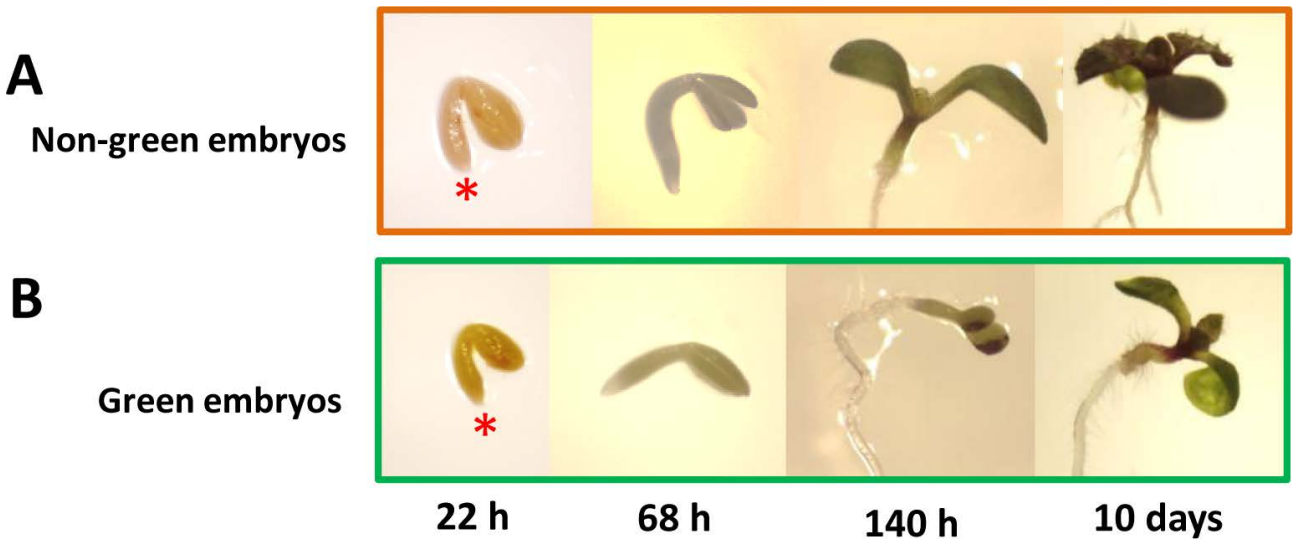

Figure S7. Seedlings developing from green embryos are viable.

A, B. Monitoring of seedlings developing from non-green (A) and green (B) mature embryo in the light. Red star indicates a root pole. Time in hours/days after transfer for incubation.

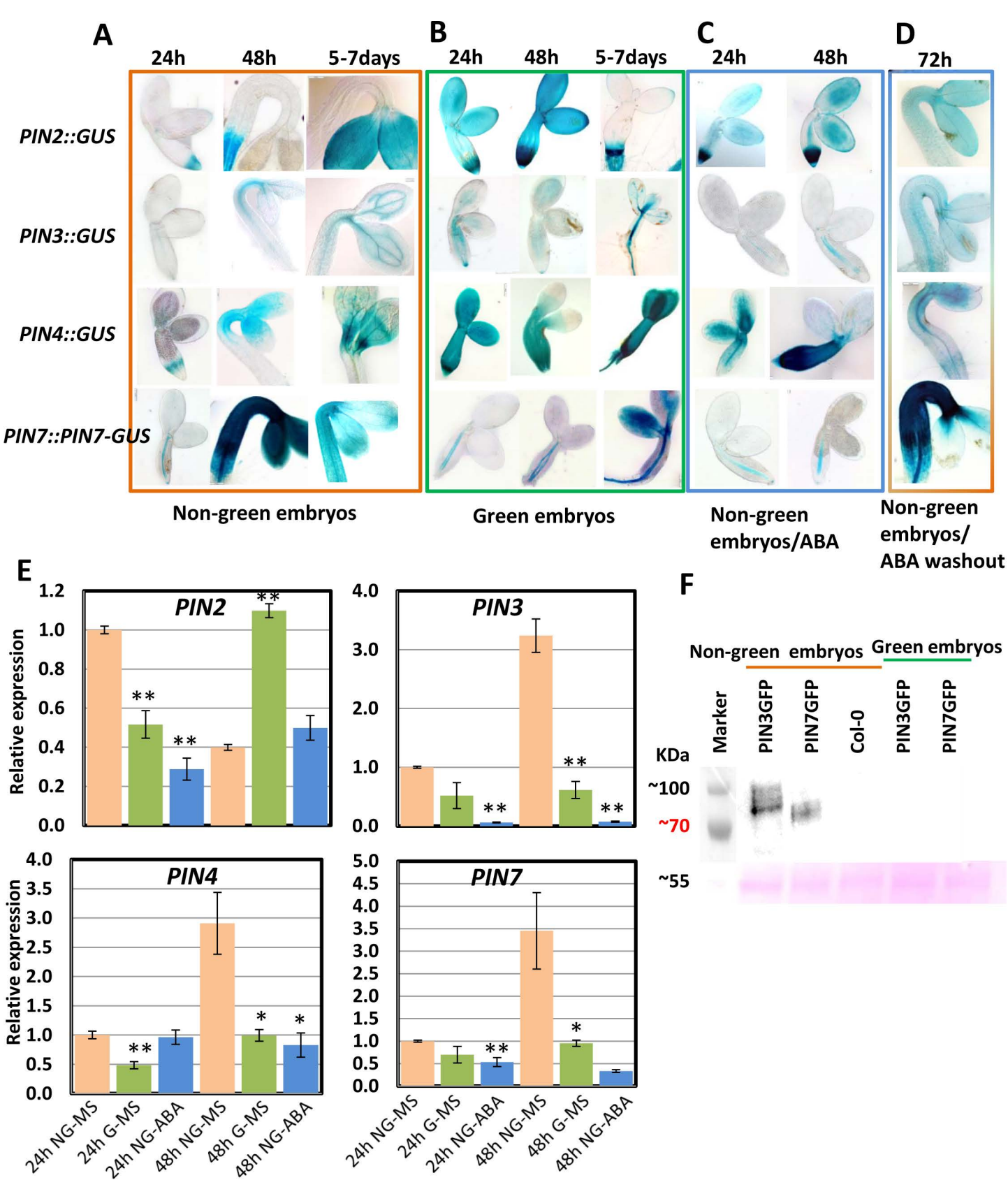

Figure S8. Monitoring of *PIN* expression in seedlings developing from green embryos and non-green embryos at presence of ABA.

A-D. Expression of *PIN:GUS* reporter lines in seedlings developing from non-green embryos (A), green embryos (B), non-green embryos at presence of 10µM ABA (C) and after ABA washout (D). Washout performed by growing seedlings for 48h on MS supplemented with 10µM ABA, followed by transfer of the seedlings back to MS media for 24h (D). Time in hours after start of incubation.

E. RT-qPCR analysis of PIN expression in seedlings developing from non-green embryos (NG, orange bar), green embryos (G, green bar) and non-green embryos treated with 10µM ABA (NG, blue bar). Time in hours after transfer for incubation. Asterisks indicate significant differences in transcript levels (Student t-test: *, $P < 0.05$; **, $P < 0.01$) between seedlings developing from green or non- green ABA treated Vs non-green embryos at the same time points. MS – Murashige and Skoog medium.

C. Analysis of PIN3-GFP and PIN7-GFP protein levels performed by Western-blot using GFP specific antibodies. Protein extracts obtained from seedlings of *PIN3:PIN3-GFP* and *PIN7:PIN7-GFP* lines developing from non- or green embryos for 72h in darkness. Expected size for PIN3-GFP is 95,5kDa and for PIN7-GFP is 93,6kDa. Ponceau staining of the membrane is shown as a loading control.

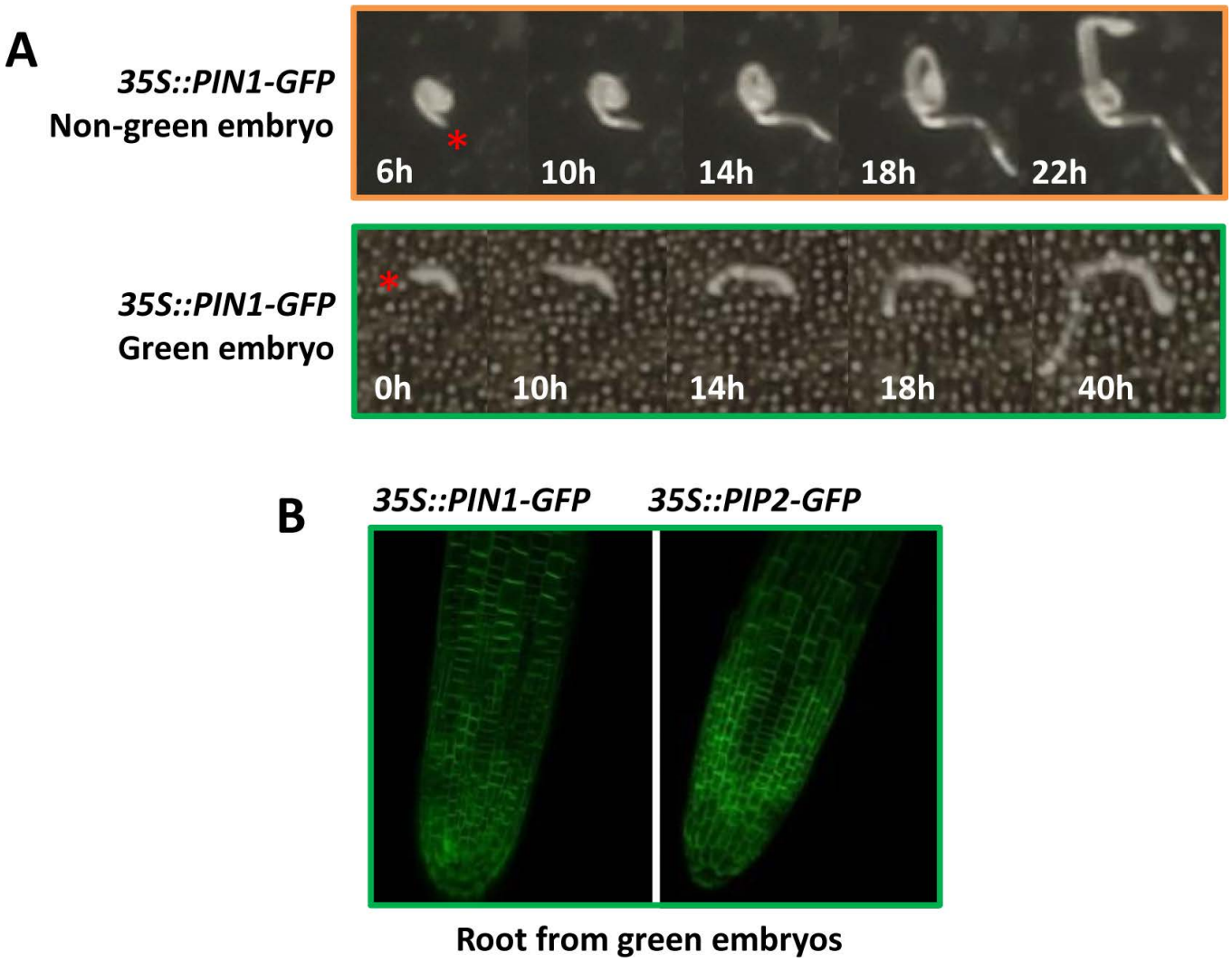

Figure S9. Ectopic expression of *PIN1* does not recover formation of the apical hook in seedlings developing from green embryos.

A. Real time monitoring of seedlings expressing PIN1-GFP under constitutive *35S* promoter, germinating from non- green and green embryos. Time in hours after germination.

B. PIN1 and PIP2 localizes to plasma membranes in root epidermal cells of *35S::PIN1-GFP* and *35S::PIP2-GFP* seedlings developing from green embryos.

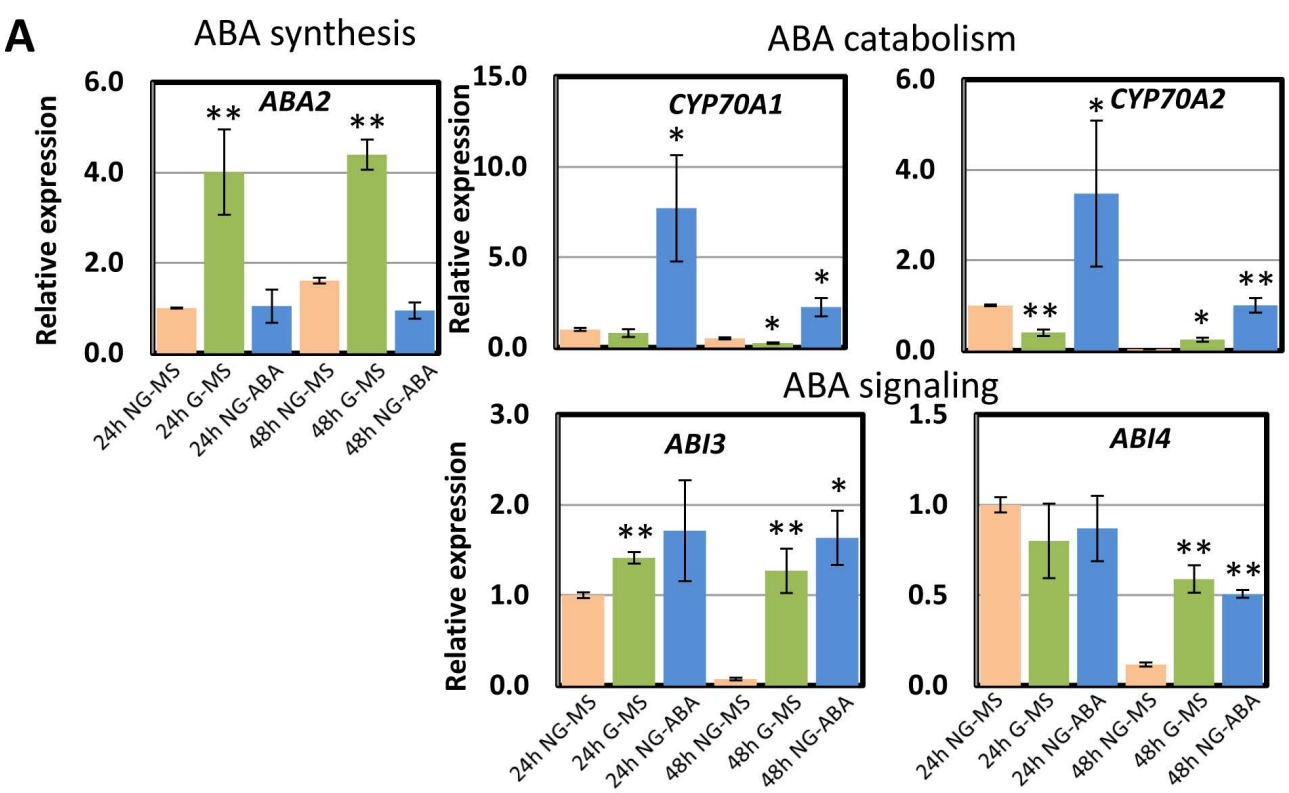

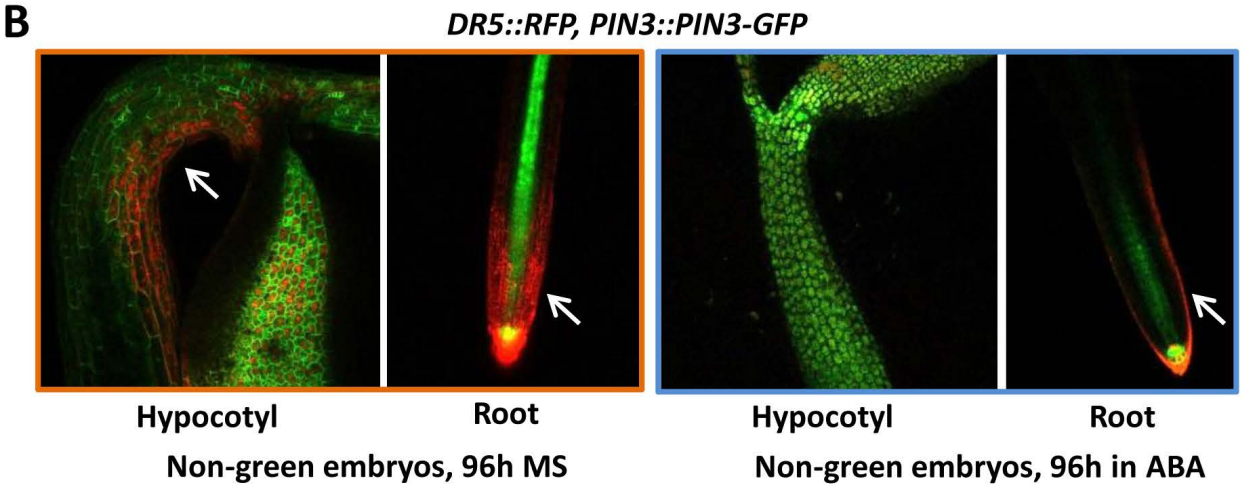

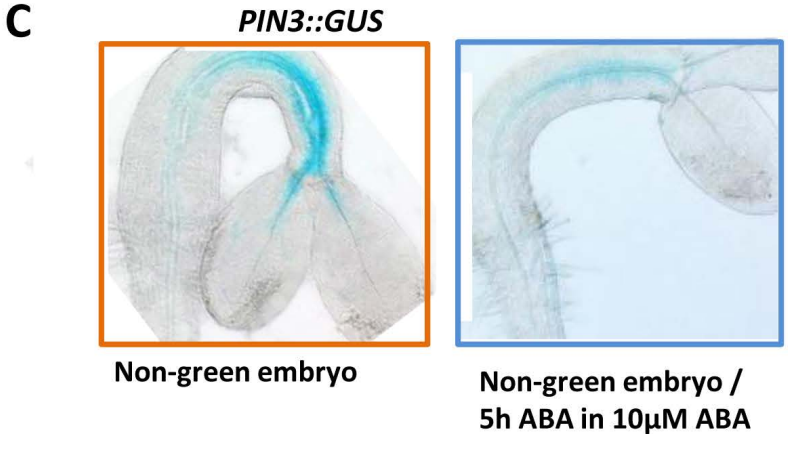

Figure S10. Development of seedlings from non-green embryos at presence of ABA mimics development of seedlings from green embryos.

A. Relative expression of ABA synthesis, catabolism and signaling genes during early stages of seedlings development from non-green embryos (NG, orange bar), green embryos (G, green bar) and non-green embryos treated with 10µM ABA (NG, blue bar). Time in hours after transfer for incubation. Asterisks indicate significant differences in transcript levels (Student t-test: *, $P < 0.05$; **, $P < 0.01$) between seedlings developing from green or non-green ABA treated Vs non-green embryos at the same time points. MS – Murashige and Skoog medium.

B. Monitoring of *DR5::RFP* auxin reporter expression during germination of seedlings from untreated and 0.1µM ABA treated non-green embryos. Reporter signal (red) is detected in the apical hook and at the root tip of untreated seedlings. In contrast, auxin maxima (red) observed in roots, but not hypocotyl of seedlings germinated from non-green embryos at presence of ABA. Green signal corresponds to *PIN3::PIN3-GFP* reporter. Time in hours after transfer for incubation. White arrows indicate auxin response maximum.

C. *PIN3::GUS* expression in seedlings treated with MS and MS supplemented with 10µM for 5 hours. MS – Murashige and Skoog medium. Experimental set up as for Figure 7B.

TABLE S1. Number of green embryos forming hook

Genotype	Col-0		
Treatment	**Seedlings wih hook**	**Seedlings without hook**	**% rescued**
AM	0	10	0.0
Abm	0	11	0.0
Abm+GA	0	12	0.0
	aba2-1		
Treatment	**Seedlings wih hook**	**Seedlings without hook**	**% rescued**
AM	0	22	0.0
Abm	1	21	**4.5**
Abm+GA	11	9	**55.0**
	Non-green embryos		
Treatment	**Seedlings wih hook**	**Seedlings without hook**	**% rescued**
AM	12	0	100.0
Abm	13	0	100.0
Abm+GA	9	0	100.0

Quantifications done from the experiment shown in Figure 8.

TABLE S2. Primers used for RT-qPCR

Name	Sequence	Gene\Seq
PIN2 F	TCACGACAACCTCGCTACTAAAGC	AT5G57090
PIN2 R	TGCCCATGTAAGGTGACTTTCCC	AT5G57090
PIN3 F	AAGGCGGAAGATCTGACCAAGG	AT1G70940
PIN3 R	TGCTGGATGAGCTACAGCTTTG	AT1G70940
PIN4 F	ACAACGTGGCAACGGAACAATC	AT2G01420
PIN4 R	GCCGATATCATCACCACCACTC	AT2G01420
PIN7 Fw	ATTGCGTGTGGCCATTGTTCAAGC	AT1G23080
PIN7 Rv	GCAACCACAAACGGCACGATCC	AT1G23080
ABI3 F	GGGAGGGACCTGGATGTATT	AT3G24650
ABI3 R	GCTCGGTCCATGGTAGGTAA	AT3G24650
ABI4 F	GTCCAGATGGGACAATTCCAACACC	AT2G40220
ABI4 R	CCCTAACGCCACCTCATGATGAAAC	AT2G40220
ABA2 F	TTCTCTTCCTAGTCAAAGGCTTT	AT1G52340
ABA2 R	GCAGACTTTGGCACCGTGCT	AT1G52340
CYP707A1-fw	TCATCTCACCACCAAGTA	AT4G19230
CYP707A1-rev	AAGGCAATTCTGTCATTCTA	AT4G19230
CYP707A2-Fw	ATCCATCACTCCTCCGAATTCTTCC	AT2G29090
CYP707A2-Rev	TCCATTTCCGAATGGCATGTACG	AT2G29090
PP2A F	TAACGTGGCCAAAATGATGC	AT1G69960
PP2A R	GTTCTCCACAACCGCTTGGT	AT1G69960

Movie 1. Apical hook development from embryos orientated in root-downwards position. Plasma membrane marker PIP2-GFP used to visualise plasma membranes.

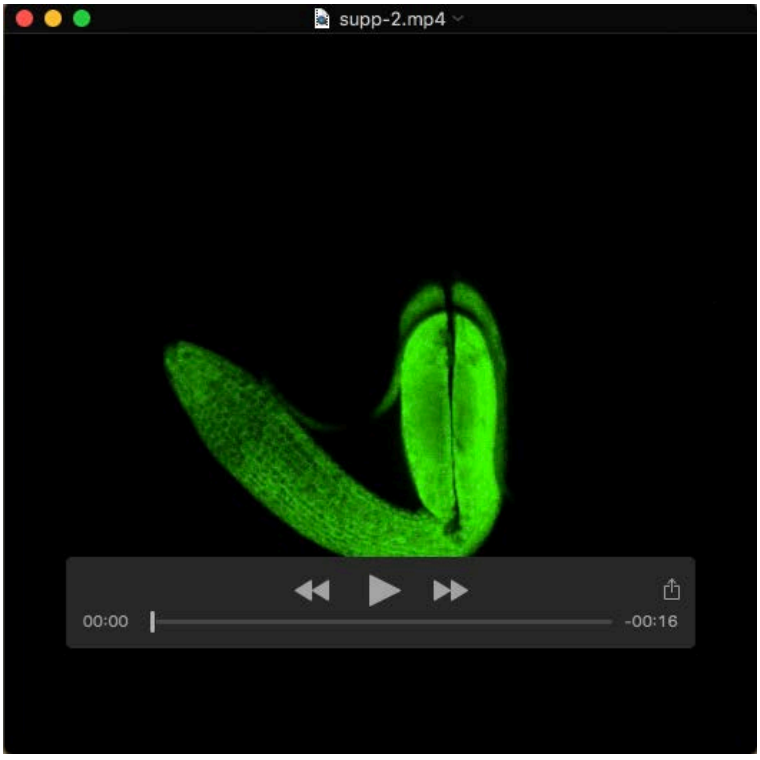

Movie 2. Apical hook development from embryos orientated in root- upwards position. Plasma membrane marker PIP2-GFP used to visualise plasma membranes.

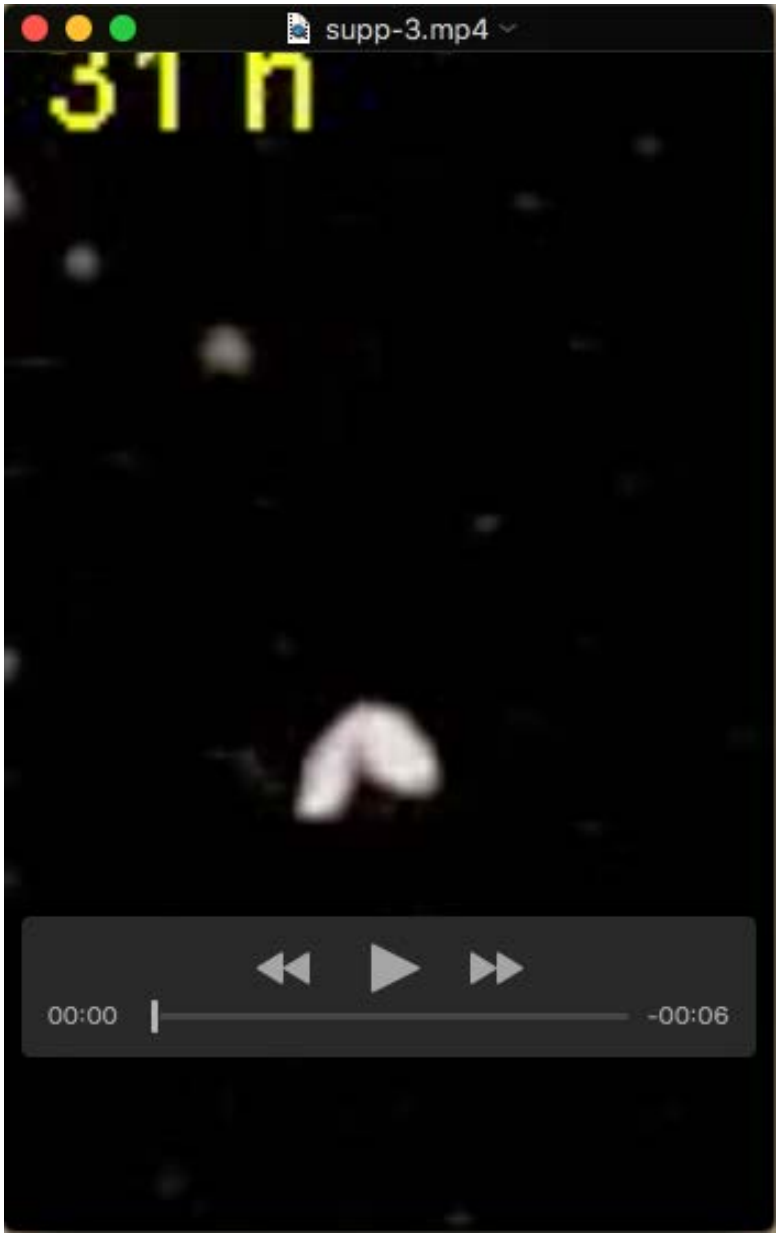

Movie 3. Apical hook development from embryos of *pin2* mutant orientated in root-downwards position.

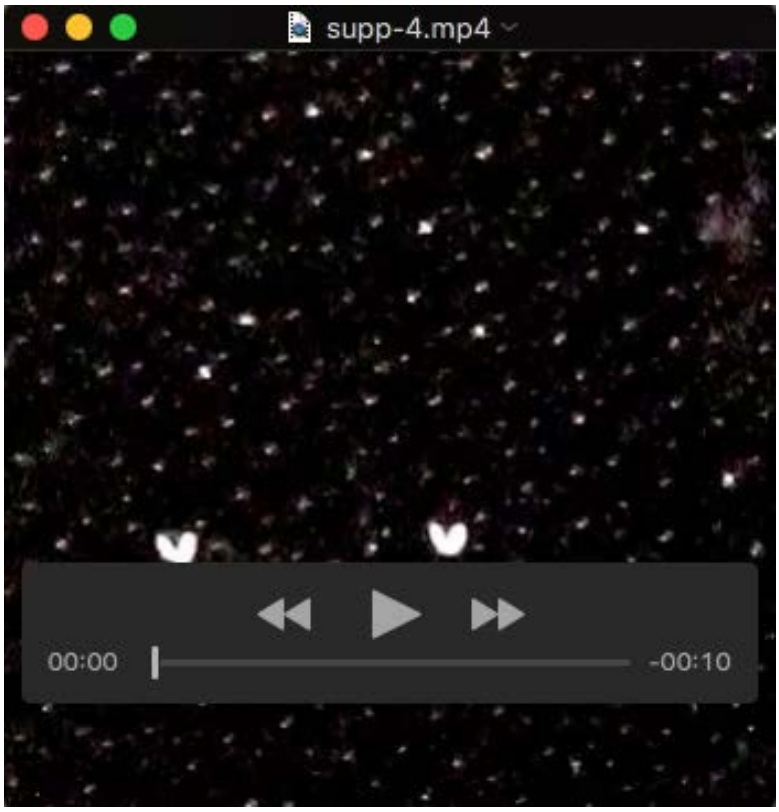

Movie 4. Apical hook development from embryos of *pin2* mutant orientated in root-upwards position.

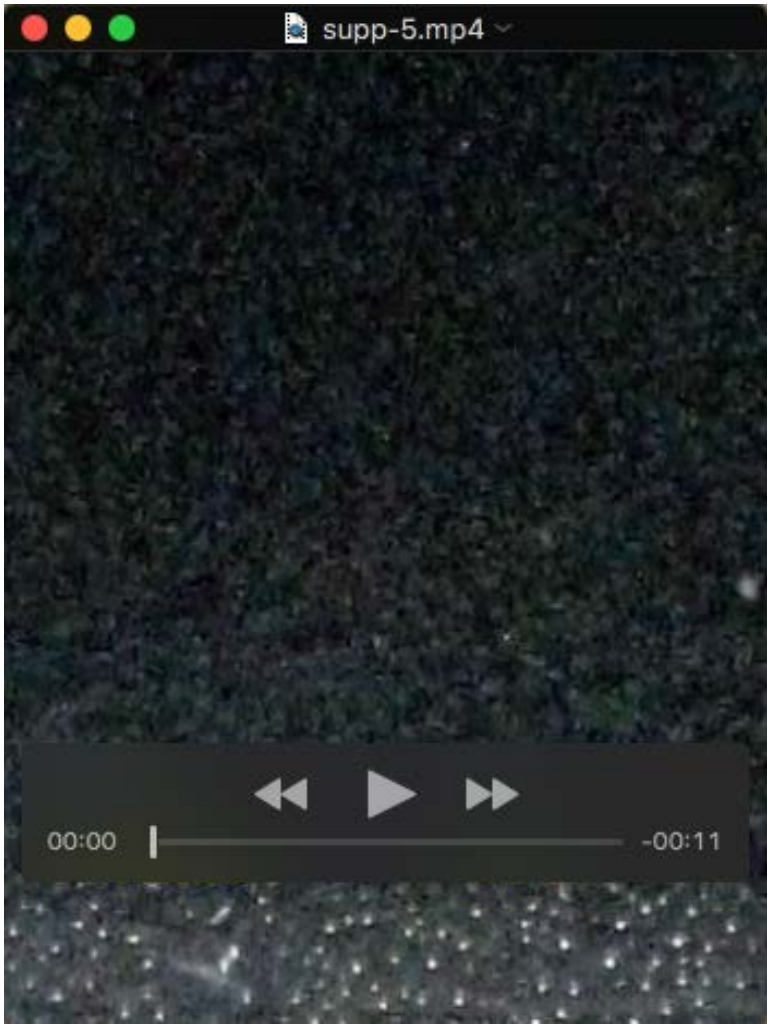

Movie 5. Apical hook development in *rml* mutant and Col-0 control.

Movie 6. Apical hook development from embryos of F1 progeny of *J0951>>UAS::AXR3*, orientated in root-downwards position.

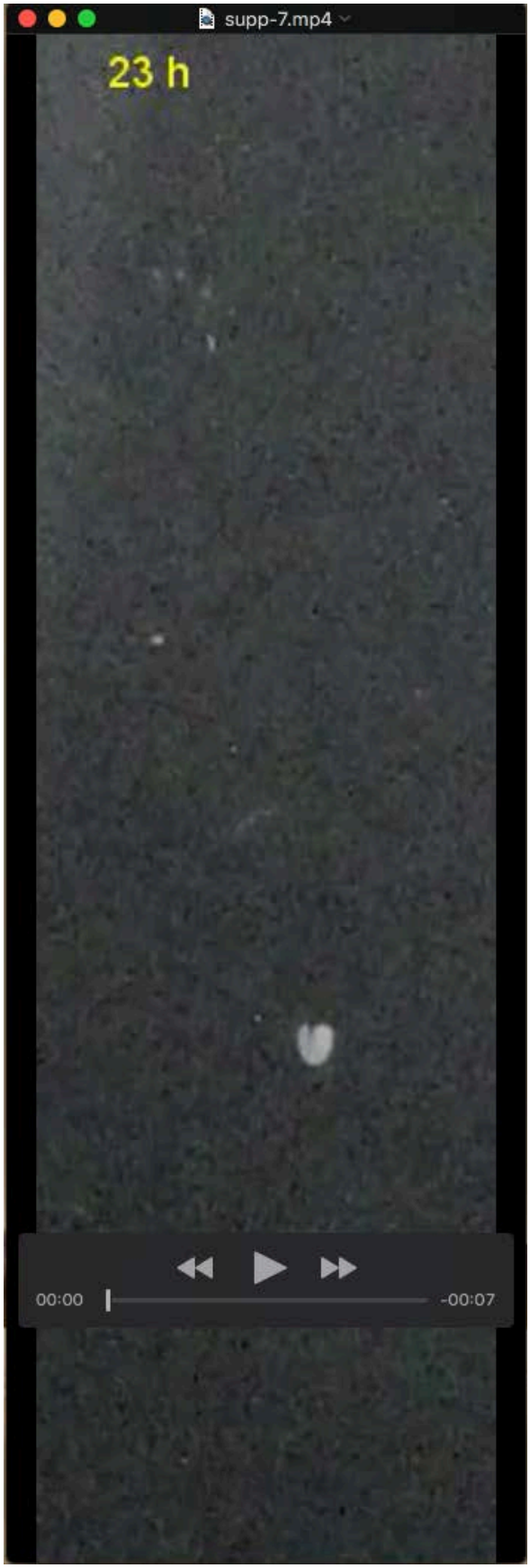

Movie 7. Apical hook development from embryos of F1 progeny of *J0951>>UAS::AXR3*, orientated in root- upwards position.

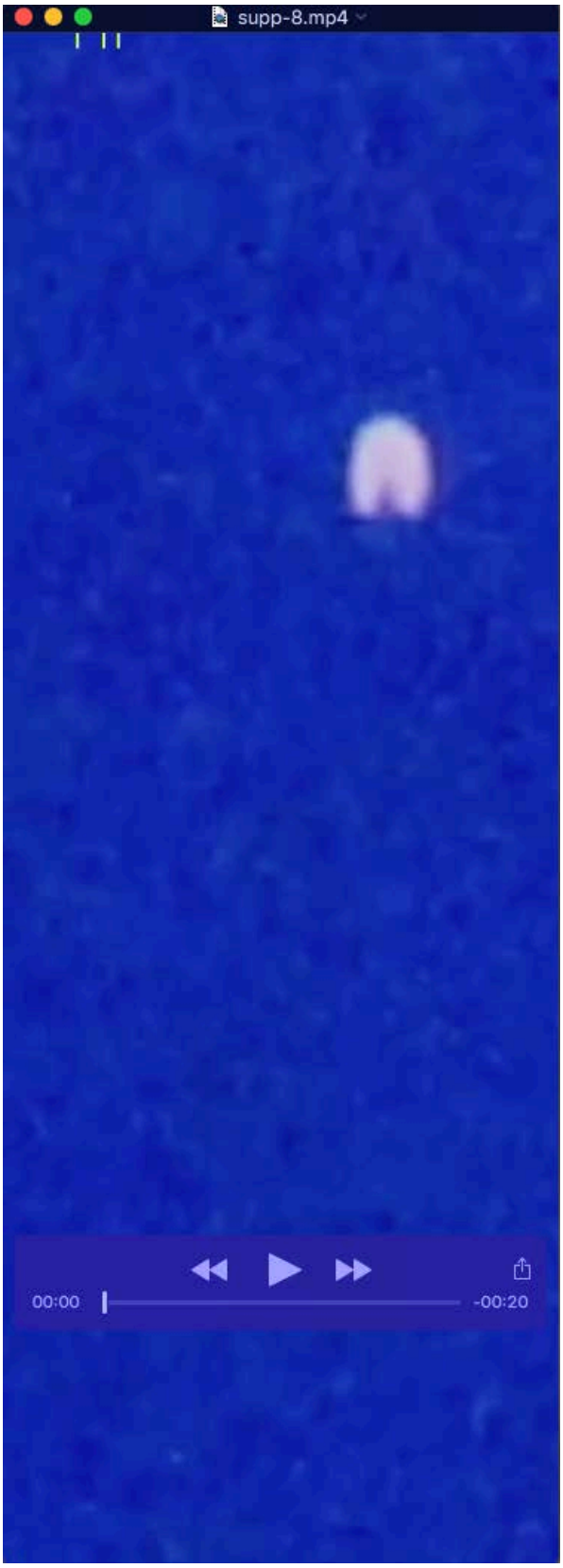

Movie 8. Apical hook development from embryos of Col-0 orientated in root-downwards position under constant light.

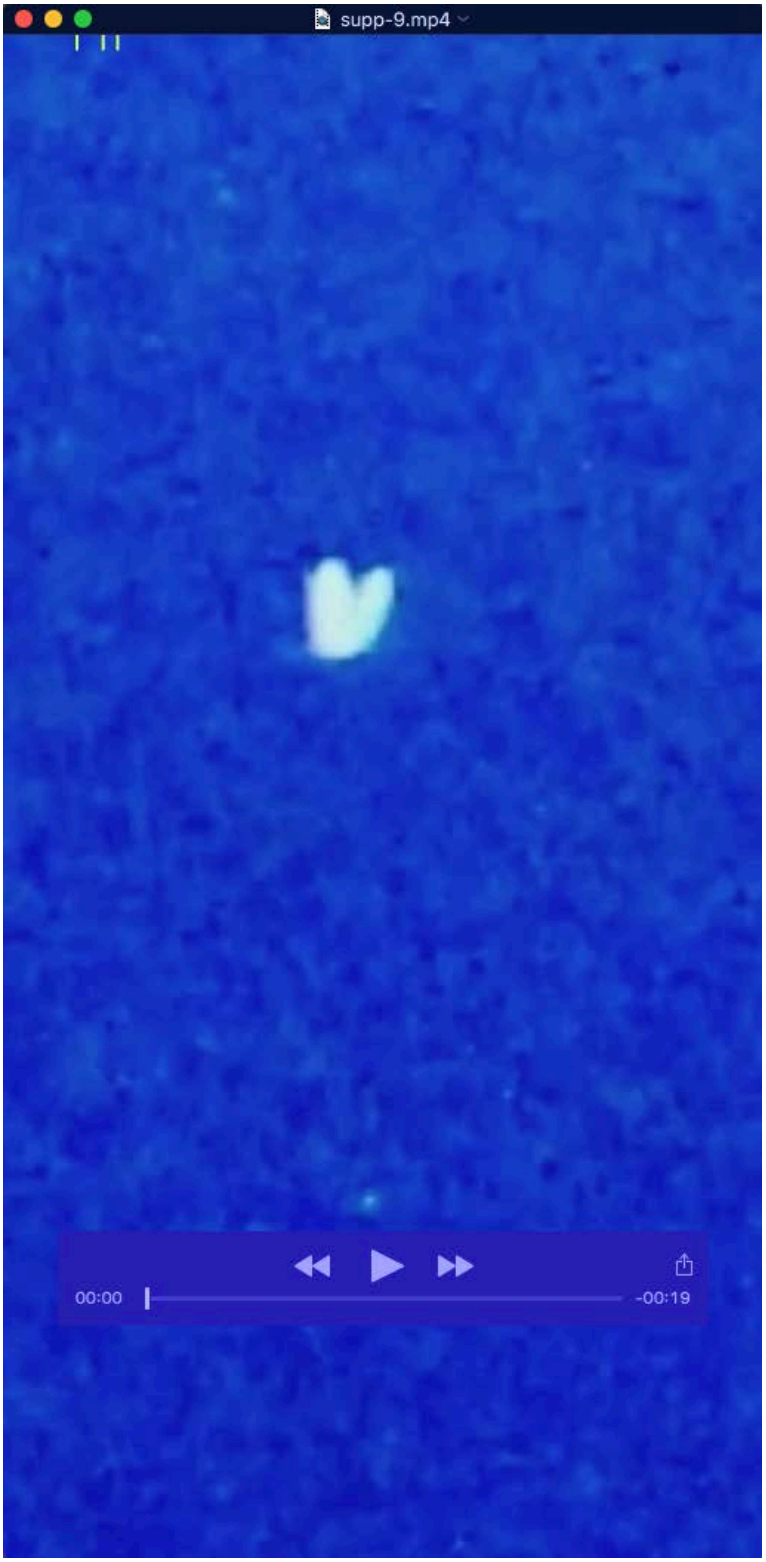

Movie 9. Apical hook development from embryos of Col-0 orientated in root- upwards position under constant light.

Movie 10. Germination of seedlings from green embryos orientated in root-downwards position, in darkness.

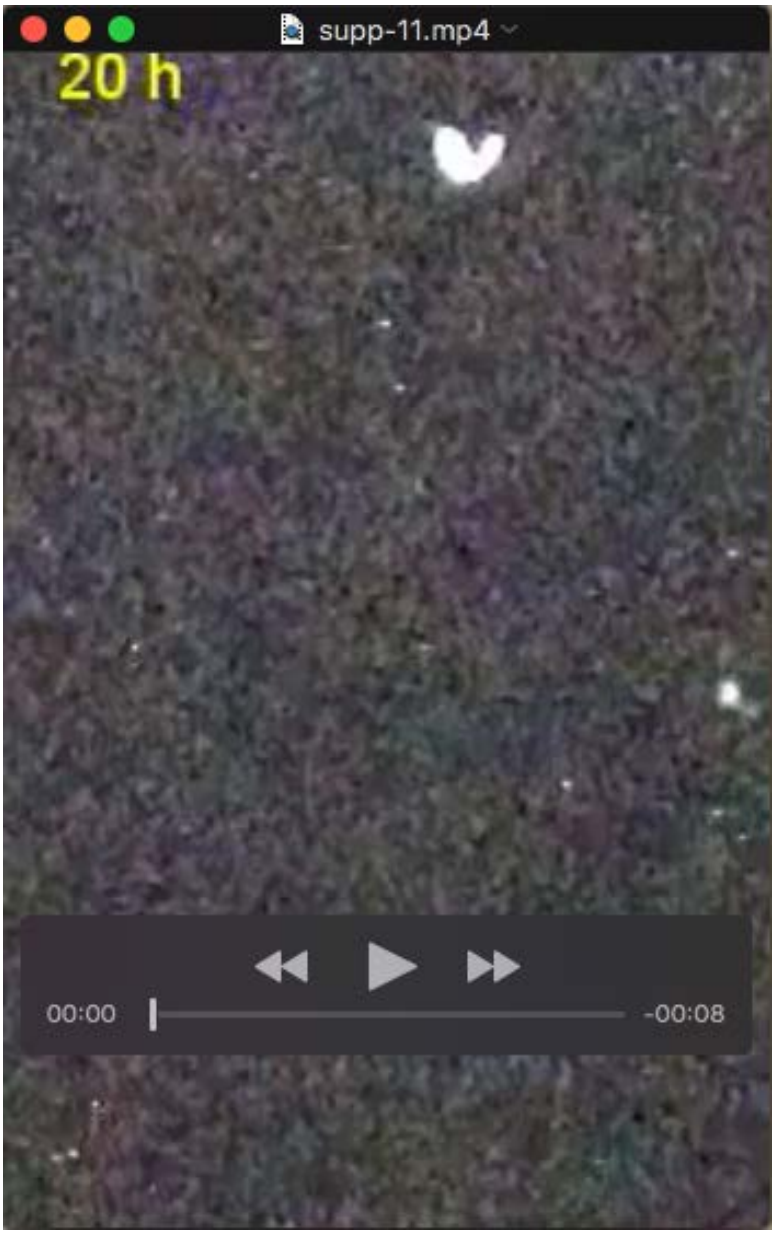

Movie 11. Germination of seedlings from green embryos orientated in root-upwards position, in darkness.